

Inference with Randomized Regression Trees

Soham Bakshi*

Department of Statistics, University of Michigan, MI, USA.

and

Yiling Huang*

Department of Statistics, University of Michigan, MI, USA.

and

Snigdha Panigrahi[†]

Department of Statistics, University of Michigan, MI, USA.

and

Walter Dempsey[‡]

Department of Biostatistics and Institute for Social Research,
University of Michigan, MI, USA.

Abstract

Regression trees are a popular machine learning algorithm that fit piecewise constant models by recursively partitioning the predictor space. In this paper, we focus on performing statistical inference in a data-dependent model obtained from the fitted tree. We introduce Randomized Regression Trees (RRT), a novel selective inference method that adds independent Gaussian noise to the gain function underlying the splitting rules of classic regression trees.

The RRT method offers several advantages. First, it utilizes the added randomization to obtain an exact pivot using the full dataset, while accounting for the data-dependent structure of the fitted tree. Second, with a small amount of randomization, the RRT method achieves predictive accuracy similar to a model trained on the entire dataset. At the same time, it provides significantly more powerful inference than data splitting methods, which rely only on a held-out portion of the data for inference. Third, unlike data splitting approaches, it yields intervals that adapt to the signal strength in the data. Our empirical analyses highlight these advantages of the RRT method and its ability to convert a purely predictive algorithm into a method capable of performing reliable and powerful inference in the tree model.

Keywords: CART, Non-linear Regression, Post-selection inference, Randomization, Regression trees, Selective inference

*Co-first authors

[†]The author acknowledges support by NSF CAREER Award DMS-2337882 and NIH grant 1R01GM152549-01.

[‡]The author acknowledges support by NIH grants 1R01GM152549-01 and 1P50DA054039-01.

1 Introduction

Regression trees are a common machine learning algorithm for non-linear regression in which regions of the predictor space \mathcal{X} are recursively partitioned into smaller regions. The outcome in these smaller regions is thought to be predicted well by a simple model [Breiman et al., 1984]. The recursive partition is typically chosen to be a binary tree and splits of the binary tree correspond to half-spaces in the predictor space. Each terminal region in the tree represents a cell of the partition, and is accompanied by its own simple model.

Splits in the tree are determined by questions about the predictor space, with branches labeled by the answers. A key feature of regression trees is that each subsequent question about the predictors, which determines downstream splits, depends on the answers to previous questions or the splits formed upstream. In classic regression trees, each such question refers to only a single predictor and the simple model in each cell is the constant model. This results in an overall model that is piecewise-constant, offering several advantages. First, predictions are fast and easy to compute. Second, piecewise constant models are good at approximating non-linear behavior. Third, these predictive models are fairly interpretable as the tree itself carries all the information necessary to tell what variables are important in forming predictions.

Despite these appealing features, classic regression trees largely remain an example of a *pure prediction algorithm* [Efron, 2020]. Such algorithms go directly for high predictive accuracy while neglecting both parameter estimation and attribution or significance of the estimated parameters in the models they fit. Efron comments on this in his article:

“the pure prediction algorithms are a powerful addition to the statistician’s armory, yet substantial further development is needed for their routine scientific applicability”.

To answer attribution questions, this paper considers surface plus noise models in the

context of regression trees where the outcome vector $Y := (Y_1, \dots, Y_n) \sim \mathcal{N}(\mu, \sigma^2 I_n)$ and μ is the unknown mean parameter. Such questions involve, for example, assessing the significance of the difference in mean response between two sibling terminal regions. Since the sequence of greedily chosen splits in the tree leading to these terminal regions are highly data dependent, naïve approaches for inference, such as Wald-type tests and intervals, cannot be used for addressing attribution questions in the fitted model.

Selective inference tools afford the ability to answer attribution questions in data-dependent models. One of the simplest selective inference tools is data splitting: divide the data into two independent subsets, and then fit a regression tree to one subset and use the second subset for inference. As an example, consider sample splitting, where the observations are partitioned into two disjoint subsets, assuming that they are independent and identically distributed. A variant of data splitting for a normal outcome vector is the *UV method* by Rasines and Young [2023], which belongs to a larger category of data fission methods [Leiner et al., 2023]. This method draws an external randomization vector $W \sim \mathcal{N}(0, \sigma^2 \gamma I_n)$ to construct a pair of independent copies of Y , i.e., $U := Y + W$, and $V := Y - \frac{1}{\gamma}W$. The regression tree algorithm uses U to build the tree, while terminal node inference proceeds with the standard Wald-type intervals using V . In practical applications, sample splitting can leave certain regions of the tree without any held-out samples. In such cases, the UV method may emerge as the preferred variant of data splitting.

A universal limitation of all data splitting approaches is the inherent trade-off between predictive modeling and inference, though. This can result in an inferior model compared to the naïve method if too little data is used for modeling, or it may produce wide intervals if too little data is saved for inference. Striking the right trade-off between the two tasks is notoriously challenging in practice. In particular, using less data at the time of modeling

might result in weak predictive accuracy, a trade-off often deemed unacceptable in applied settings [Athey and Imbens, 2016]. An alternative framework for conducting valid inference in data-dependent models, while using the full set of observations, including the data used during modeling, is conditional selective inference [Lee et al., 2016]. This approach conditions on the output of the selection process and produces intervals that, unlike data splitting, adapt to the amount of signal in the data, reverting to standard intervals in the absence of selection. Neufeld et al. [2022] introduced such an approach for regression trees called *Tree-Values*, which uses the full dataset for both fitting the regression tree and conducting inference on data-dependent parameters. Although this method achieves nominal coverage rate, it can still produce very wide intervals for certain parameters.

In this paper, we introduce a conditional selective inference methodology relying on a novel randomization scheme that adds independent Gaussian noise to the gain function underlying the splitting rule of classic regression trees. Based on this, we refer to our proposal as *Randomized Regression Trees (RRT)*. Similarly to data splitting, the added Gaussian randomization provides the analyst with a flexible lever to choose the amount of data used for modeling versus inference, enabling a trade-off between the predictive accuracy of the model and inferential reliability and power in the fitted model. At the same time, our method utilizes randomization to overcome the limitations of both data splitting approaches and the existing *Tree-Values* method:

- Specifically, we show that introducing a small amount of randomization to the gain function allows us to fit a tree model using almost the entire dataset, effectively mimicking the model fit with naïve method. Unlike data splitting, however, our approach then utilizes the full dataset for inference resulting in much shorter intervals than inference on the held-out portion.

- Our intervals, similar to those from conditional methods, adapt to the amount of signal in the data, i.e., our intervals widen or narrow depending on the strength of the effect of selection. Furthermore, even with a small amount of randomization, our method produces significantly shorter intervals compared to the Tree-Values method, which does not use external randomization.

These practical advantages of our method over existing methods are reinforced in the next section through a first example.

1.1 First example

We consider a simple surface plus noise example using data generated in a similar fashion to Neufeld et al. [2022]. Let $X \in \mathbb{R}^{n \times p}$ with $n = 200, p = 5, X_{ij} \stackrel{i.i.d.}{\sim} \mathcal{N}(0, 1)$, and $Y \sim \mathcal{N}_n(\mu, \sigma^2 I_n)$ with $\sigma = 2$. The vector μ with $(\mu)_i = b \times [1_{(x_{i,1} \leq 0)} \times \{1 + a1_{(x_{i,2} > 0)} + 1_{(x_{i,3} \times x_{i,2} > 0)}\}]$ defines a three-level tree where $a = 1, b = 2$ determine the signal strength.

We consider our proposed RRT method and three baseline methods: (1) naïve inference, (2) UV method (or Data Fission for normal data), (3) Tree-Values method. For each method, the maximum depth of the final tree is 3, the minimum number of samples in a node to be split is 25, the minimum size of terminal nodes is 10, and we do not prune after the stopping criteria is met. After estimating the trees, confidence intervals for terminal regions are computed and evaluated based on three metrics: (1) coverage rate, (2) average confidence interval length, and (3) test mean squared error (MSE).

To start, we compare the two non-randomized inference methods, naïve and Tree-values, to our proposed method on the same simulated dataset over 500 simulations. In our RRT proposal, the randomization sd τ , specified in Section 5, takes 5 distinct values, corresponding to 5 levels of randomization: RRT(1), RRT(2), ..., RRT(5). Among these,

RRT(1) represents the method with the least amount of randomization. Figure 1 presents the results. Both RRT and Tree-Values achieve valid 90% coverage, while naïve inference fails to deliver valid coverage. Tree-Values lead to very wide confidence intervals, whereas RRT, at all levels of randomization, produce significantly shorter intervals. Finally, in terms of predictive accuracy, RRT(1) achieves comparable test MSE as the non-randomized methods. With a small amount of randomization, RRT converts a *pure prediction algorithm* into a method that achieves high predictive accuracy while also answering questions of attribution in surface plus noise models with high inferential power.

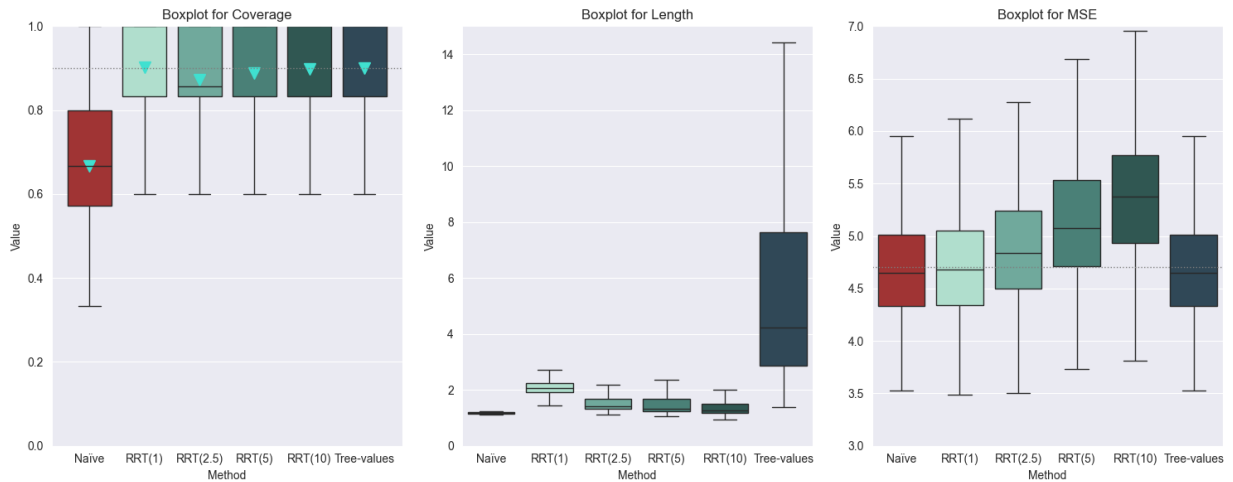


Figure 1: Coverage rate, average CI length, and prediction MSE of the proposed method, Tree-Values, and Naïve; The dotted line is plotted at 0.9 in the coverage plot, and at the mean value of the proposed method in the MSE plot; Triangles in the coverage plot indicates the empirical averages of coverage rates

We next compare RRT(1), which achieves similar predictive accuracy as the naïve method, to the UV method with $\gamma \in \{0.1, 0.2, 0.3, 0.4, 0.5\}$, on the same simulated dataset. Figure 2 presents the results for 500 simulations. Both methods achieve 90% nominal coverage. Though, there is a clear trade-off between attribution and predictive accuracy for the UV method. To achieve similar interval lengths to RRT(1), UV sacrifices predictive accuracy (see, for example, UV(0.5)). To achieve similar predictive accuracy to RRT(1)

(see, for example, $UV(0.1)$), it produces confidence intervals that are nearly twice as wide.

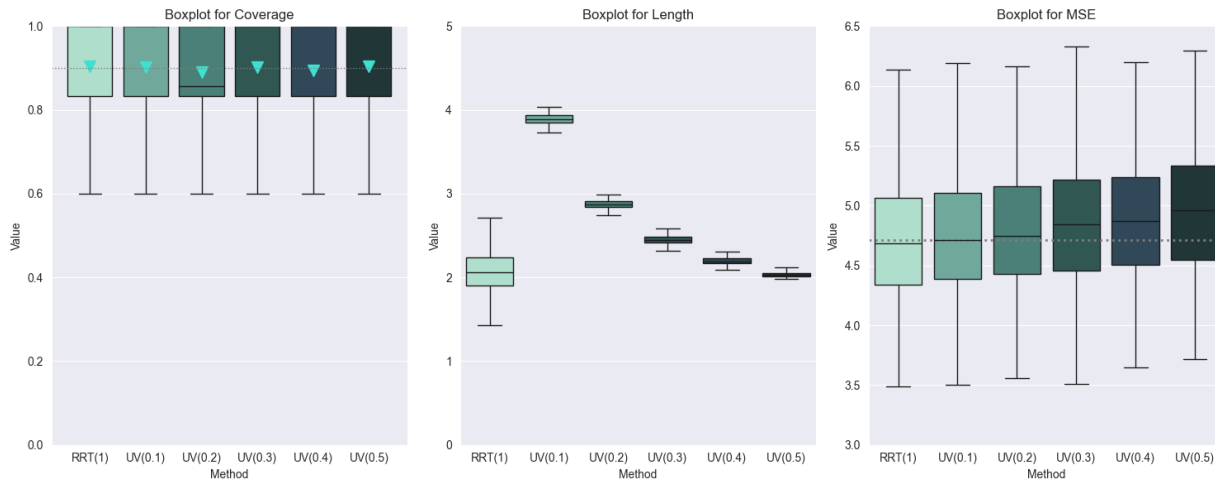


Figure 2: Coverage rate, average CI length, and prediction MSE of the proposed method and the UV method; The dotted line is plotted at 0.9 in the coverage plot, and at the mean value of “Naïve” in the MSE plot; Triangles in the coverage plot indicates the empirical averages of coverage rates

The rest of this paper is organized as follows. In Section 2, we review related work and fix some notations relevant to regression trees. In Section 3, we present our randomized CART algorithm and provide a preview of our main idea of inference using randomization. In Section 4, we present the main results that lead to an exact, closed-form pivot for constructing selective inference using RRT. In Section 5 we investigate the performance of our new method via more extensive simulations. In Section 6, we apply our method to a mobile health (mHealth) intervention trial focused on improving health outcomes through the use of mobile health technologies. A brief summary of our contributions is presented in Section 7. All proofs and technical details are in the Supplementary Material.

2 Related work

In this section, we review other related work on selective inference and regression trees, and introduce some basic notation relevant to these trees.

Selective inference or post-selection inference. Selective inference tools enable addressing modern inference questions involving data-dependent parameters. Among these tools, conditional methods have emerged as a practical approach for controlling the nominal coverage rates. Some of these methods also ensure global error guarantees over the selected parameters, such as the false coverage rate (FCR) [Benjamini and Yekutieli, 2005]. For example, Goeman and Solari [2024] discuss the FCR, a conditional version of FCR, and highlight its distinction from nominal inferential guarantees in their paper. Lee et al. [2016] introduced the polyhedral method, a conditional approach for inference after lasso, which uses the polyhedral shape of the selection event. The conditional approach has been developed for a wide range of data-dependent inferential tasks like AIC-based model selection Charkhi and Claeskens [2018], effect modification Zhao et al. [2021], adaptive and group lasso selection Pirenne and Claeskens [2024], clustering Gao et al. [2024], and PCA Perry et al. [2024]. However, it is well known that these methods can suffer from extremely low power (i.e., infinitely wide intervals) if the observed data falls near the boundary of the selection event. This observation has been formalized for polyhedral-shaped events in Kivaranovic and Leeb [2021].

Selective inference via randomization. Introducing randomization during selection and conditioning on its output, as shown in Tian and Taylor [2018], produces more powerful inference than the polyhedral method. However, the pivot proposed in this work is not available in closed form, posing challenges for practical implementation of the method. In high-dimensional regression, randomized methods introduced in Panigrahi and Taylor

[2023], Liu [2023], Panigrahi et al. [2024] add independent Gaussian noise to the penalized estimation objective, providing computationally efficient tools for constructing randomized inference in post-selection models. Unlike data splitting, these methods use the full data for inference and produce much shorter intervals than those from the held-out portion.

The benefits of randomized methods extend beyond the power gains achieved through external randomization, as demonstrated by several recent papers. For instance, Panigrahi [2023] show that incorporating Gaussian randomization ensures valid asymptotic selective inference across various data types, including those beyond normal data. Using a similar form of randomization, Bakshi et al. [2024] develop asymptotic semiparametric selective inference for effect moderation problems. By incorporating external randomization, a recent body of work has made selective inference feasible in problems where the selection event is no longer polyhedral, and where conditional methods without randomization fail to provide easy to compute, tractable inference. Examples include selective inference for selected groups of variables [Panigrahi et al., 2023, Huang et al., 2023b] and inference for edge parameters in conditional dependence graphs [Huang et al., 2023a]. Similar to this line of work, our proposal uses a novel randomization scheme to obtain an exact, closed-form pivot that accounts for the complex selection of splits leading to the tree fit.

Regression trees. The classification and regression trees (CART) is a decision-tree algorithm that builds a tree-like structure using splitting criteria and a pruning strategy to prevent overfitting. A model-based alternative called CTree was introduced by Torsten Hothorn and Zeileis [2006] in which the tree-growing algorithm grows by hypothesis testing. CTree was designed to alleviate issues of instability and variable selection bias associated with CART. While it employs hypothesis testing for constructing a tree model, it does not address attribution questions in the model fitted by the tree algorithm.

In terms of previous inferential work on regression trees, Wager and Walther [2016] developed convergence guarantees for unpruned CART trees; however, these do not provide finite-sample results and cannot accommodate pruning. Loh et al. [2018] develop bootstrap calibration procedures that attempt to provide confidence intervals for the regions of a regression tree. However, this approach has been empirically shown to fail in providing intervals that achieve nominal coverage.

Notations. Consider a continuous response $Y \in \mathbb{R}^n$ and a set of p predictors measured on n observations, $X = (X^1, \dots, X^p)$, where $X^j \in \mathbb{R}^n$ denotes the j -th predictor. For a region $\mathcal{R} \subseteq \mathbb{R}^p$, let $n_{\mathcal{R}} = |\{i \in [n] : X_i \in \mathcal{R}\}|$ be the number of observations whose predictors fall within \mathcal{R} and let $\bar{Y}_{\mathcal{R}}$ be the mean of these observations.

A standard TREE growing algorithm starts with the entire covariate space \mathbb{R}^p , which we denote as P_1 . The algorithm then recursively partitions this space with the goal of maximizing a certain notion of “information gain” based on the data Y . Many popular tree-growing methods, including the CART, construct these partitions using a series of greedily selected recursive splits. Our focus in this paper is on recursive binary split-based methods. Splits take the form $s = (j, o) \in \mathcal{X} = [p] \times [n - 1]$ where $j \in [p]$ denotes the index of the predictor selected for splitting and o denotes the order statistic of this predictor.

For a non-terminal region $P \subseteq \mathbb{R}^p$, let $\mathcal{X}_P \subseteq \mathcal{X}$ denote the set of all possible splits that can be made on the region P . Each split $s \in \mathcal{X}_P$ partitions P into two half-spaces, $P_s^l = \{z \in \mathbb{R}^p : (z)_j \leq X_{(o)}^j\}$, $P_s^r = \{z \in \mathbb{R}^p : (z)_j > X_{(o)}^j\}$, where $(z)_j$ is the j -th coordinate of z and $X_{(o)}^j$ is the o -th order statistic of the predictor X^j . This split s is associated with a measure of information gain, denoted by $G(Y; P, s)$. In particular, the CART algorithm

selects a split s that maximizes the reduction in mean squared error (MSE)

$$G(Y; P, s) = \frac{1}{\sqrt{n_P}} \left[\sum_{i: X_i \in P} (Y_i - \bar{Y}_P)^2 - \left\{ \sum_{i: X_i \in P_s^l} (Y_i - \bar{Y}_{P_s^l})^2 + \sum_{i: X_i \in P_s^r} (Y_i - \bar{Y}_{P_s^r})^2 \right\} \right].$$

Equivalently, on each parent region P , it selects the optimal split as follows

$$s^* = \operatorname{argmax}_{s \in \chi_P} G(Y; P, s) \equiv \operatorname{argmax}_{s \in \chi_P} \frac{1}{\sqrt{n_P}} \left\{ n_{P_s^l} \bar{Y}_{P_s^l}^2 + n_{P_s^r} \bar{Y}_{P_s^r}^2 \right\}.$$

3 RRT model fit and inference preview

3.1 RRT algorithm

To grow a randomized regression tree (RRT), we add simple independent normal random variables to the gain function at each split. Specifically, for a parent region P , we maximize a randomized gain function to select the split s^* from the set of possible splits χ_P as:

$$s^* = \operatorname{argmax}_{s \in \chi_P} G(Y; P, s) + W(s),$$

where the external randomization variables $W(s) \sim \mathcal{N}(0, \tau_P^2)$ are independent of Y and of each other, both at the same split and across different splits within the tree algorithm. Algorithm 1 outlines our procedure for constructing a RRT with a maximum depth d_{\max} . In the special case where $W(s) = 0$, i.e., no randomization, the standard CART algorithm is recovered.

Algorithm 1 Randomized CART: fixed depth TREE growing algorithm

- 1: **Input:** Training data (X, Y) , maximum depth d_{\max}
 - 2: **Initialize:** Root region $P_1 = \mathbb{R}^p$, current depth $d = 0$
 - 3: **for** each region P with n_P samples at depth d **do**
 - 4: **if** $d < d_{\max}$ and $n_P > 1$ **then**
 - 5: Compute the gain function $G(Y; P, s)$ for all possible splits $s = (j, o) \in \chi_P$
 - 6: Draw a data-independent randomization $W(s) \sim \mathcal{N}(0, \tau_P^2)$ for all $s \in \chi_P$
 - 7: Select the split s^* with the maximum randomized gain:
$$s^* = \operatorname{argmax}_{s \in \chi_P} G(Y; P, s) + W(s)$$
 - 8: Partition P based on selected split into $\{P_{s^*}^l, P_{s^*}^g\}$
 - 9: depth $d \leftarrow d + 1$
 - 10: **else**
 - 11: Return P as a terminal region
 - 12: **end if**
 - 13: **end for**
-

3.2 TREE-model

Introducing some notations, let \bar{S} denote the collection of all splits generated by the RRT Algorithm 1, and let \bar{W} collect all the external randomization variables added to the gain functions to obtain the splits in \bar{S} . The output of the RRT algorithm, denoted as $\text{TREE}(Y, \bar{W}) = \bar{R} = \{R_1, R_2, \dots, R_M\}$, is the set of terminal regions in the tree, also called leaves. Furthermore, let $\bar{P} = \{P_1 = \mathbb{R}^p, \dots, P_K\}$ denote all the internal or non-terminal regions in this tree output.

Suppose for our observed realization of the data $Y = y$, the M terminal regions observed as output of the RRT algorithm are $\{R_1 = \mathcal{R}_1, R_2 = \mathcal{R}_2, \dots, R_M = \mathcal{R}_M\}$. Associated with this output, a predictive TREE-model for the RRT is given by:

$$Y \sim \mathcal{N}(\mu, \sigma^2 I_n), \text{ where } (\mu)_i = \sum_{m=1}^M \mu_{\mathcal{R}_m} \mathbb{1}[X_i \in \mathcal{R}_m], \forall i \in [n], \quad (1)$$

where X_i represents the i -th observed value for the p predictors. Note that the M parameters $\{\mu_{\mathcal{R}_1}, \mu_{\mathcal{R}_2}, \dots, \mu_{\mathcal{R}_m}\}$ in this TREE-model depend on the data and the externally added randomization variables through the splits generated during the tree-growing process of the RRT algorithm.

Conducting inference in the TREE-model described in (1) is a natural step. One common task is performing inference on the model parameters $\mu_{\mathcal{R}}$, for $\mathcal{R} \in \overline{\mathcal{R}}$, where $\overline{\mathcal{R}}$ is the observed value of \overline{R} . Another task is comparing differences between the mean parameters of two sibling regions within the tree, $\mu_{\mathcal{R}} - \mu_{\mathcal{R}'}$, if \mathcal{R} and \mathcal{R}' are two sibling regions in the TREE-model. As emphasized earlier, none of these tasks can be addressed with naïve inference, due to the complex dependence between the TREE-model and our data.

3.3 Conditional inference and guarantees

For now, suppose that we focus on inference for the mean parameter associated with the terminal region $\mathcal{R} \in \overline{\mathcal{R}}$. Let $\nu_{\mathcal{R}}$ be an n -dimensional vector such that

$$(\nu_{\mathcal{R}})_i = \frac{\mathbb{1}[X_i \in \mathcal{R}]}{\sqrt{n_{\mathcal{R}}}}.$$

Naïve inference for $\mu_{\mathcal{R}}$ relies on the normal distribution of the Wald test-statistic $\sqrt{n_{\mathcal{R}}}\overline{Y}_{\mathcal{R}} = \nu_{\mathcal{R}}^{\top}Y$, which is based on the mean of the observations in \mathcal{R} . Obviously, this distribution ignores the data-dependent nature of the TREE-model.

Following the principles of conditional inference, we base inference on the conditional distribution of

$$\nu_{\mathcal{R}}^{\top}Y \mid P_{\nu_{\mathcal{R}}}^{\perp}Y = P_{\nu_{\mathcal{R}}}^{\perp}y, \overline{S} = \overline{s}, \quad (2)$$

where \overline{S} is the collection of all splits in $\text{TREE}(Y, \overline{W})$ and

$$P_\nu^\perp Y = \left(I_n - \frac{\nu\nu^\top}{\|\nu\|_2^2} \right) Y.$$

Conditioning on the event $\{\overline{S} = \overline{s}\}$ takes into account the selection of the splits that lead to the terminal region \mathcal{R} , while conditioning on $\{P_{\nu_{\mathcal{R}}}^\perp Y = P_{\nu_{\mathcal{R}}}^\perp y\}$ removes nuisance parameters from this distribution, yielding a closed-form exact pivot to infer for $\mu_{\mathcal{R}}$.

This pivot facilitates the construction of selective confidence intervals $\{\widehat{C}_{\mathcal{R}} : \mathcal{R} \in \overline{\mathcal{R}}\}$, where $\widehat{C}_{\mathcal{R}}$ is the interval estimate for $\mu_{\mathcal{R}}$. Noting that $\{\overline{S} = \overline{s}\} \subseteq \{R_1 = \mathcal{R}_1, \dots, R_M = \mathcal{R}_M\} = \{\overline{R} = \overline{\mathcal{R}}\}$, the simple rationale behind conditioning on the splits is:

$$\begin{aligned} \mathbb{P} \left[\mu_{\mathcal{R}} \in \widehat{C}_{\mathcal{R}} \mid \overline{S} = \overline{s} \right] \geq 1 - \alpha &\implies \mathbb{P} \left[\mu_{\mathcal{R}} \in \widehat{C}_{\mathcal{R}} \mid \overline{R} = \overline{\mathcal{R}} \right] \geq 1 - \alpha \\ &\implies \mathbb{P} \left[\mu_{\mathcal{R}} \in \widehat{C}_{\mathcal{R}} \right] \geq 1 - \alpha. \end{aligned} \tag{3}$$

The implications in (3) are a direct consequence of the tower property of expectation. Obviously, the conditional guarantee on the left-hand side ensures coverage at the desired level for each individual post-selection parameter $\mu_{\mathcal{R}}$ for $\mathcal{R} \in \overline{\mathcal{R}}$. Moreover, following the same argument as Lee et al. [2016], it also controls the false coverage rate (FCR), defined in Benjamini and Yekutieli [2005], at level α , i.e.,

$$\text{FCR} = \mathbb{E} \left[\frac{\left| \left\{ j \in [M] : \mu_{\mathcal{R}_j} \notin \widehat{C}_{\mu_{\mathcal{R}_j}} \right\} \right|}{\max(M, 1)} \right] \leq \alpha.$$

3.4 Preview of our main idea

Before developing our inferential framework for RRT, we first illustrate our main idea of inference using a simple one-depth tree. We motivate our novel randomization approach

and demonstrate how it enables easily tractable conditional inference through this simple example. We consider the TREE-model in (1) with exactly two terminal regions, $\mathcal{R}_1 = \mathcal{R}$ and $\mathcal{R}_2 = \mathcal{R}^c$, which are the result of a single split generated by $\text{TREE}(Y, \overline{W})$. Here, $\overline{W} = \overline{W}_1$ denotes the randomization variables added to the gain functions at this first split. As before, we consider inference for $\mu_{\mathcal{R}}$, where $\mathcal{R} \in \{\mathcal{R}_1, \mathcal{R}_2\}$.

Fixing some more notations, let $\chi_{\mathcal{R},1} = \chi_1$ denote the set of possible splits for the parent region $P_1 = \mathbb{R}^p$ and let $|\chi_{\mathcal{R},1}| = d_1$. Let $S_{\mathcal{R},1}^* = S_{\mathcal{R},1}^*(Y, \overline{W}_1)$, a function of both Y and \overline{W}_1 , denote the first random split selected from this set that resulted in the region \mathcal{R} . Say that we observe the event $\{S_{\mathcal{R},1}^* = s_{\mathcal{R},1}^*\}$. In this case, a pivot is obtained from the distribution in (2) where the conditioning event is $\{\overline{S} = \overline{s}\} = \{S_{\mathcal{R},1}^* = s_{\mathcal{R},1}^*\}$. In the rest of this section, we guide our readers through the main steps of characterizing this conditional distribution.

Observe that we can express $Y = \frac{\nu}{\|\nu\|_2^2}(\nu^\top Y) + P_\nu^\perp Y$, where $\nu^\top Y$ and $P_\nu^\perp Y$ are independent variables, i.e., $\nu^\top Y \perp\!\!\!\perp P_\nu^\perp Y$. Let $\nu = \nu_{\mathcal{R}}$, where $\nu_{\mathcal{R}}$ is defined in the previous section. As a result, the random split $S_{\mathcal{R},1}^*$, made on the parent region P_1 is fully determined by the data variables $\nu_{\mathcal{R}}^\top Y$, $P_{\nu_{\mathcal{R}}}^\perp Y$, and the randomization variables \overline{W}_1 , i.e., $S_{\mathcal{R},1}^* = S_{\mathcal{R},1}^*(\nu_{\mathcal{R}}^\top Y, P_{\nu_{\mathcal{R}}}^\perp Y, \overline{W}_1)$.

With details deferred to the next section, it follows that the conditional distribution of interest has a density at $t \in \mathbb{R}$ proportional to:

$$\phi(t; \nu_{\mathcal{R}}^\top \mu, \sigma^2 \|\nu_{\mathcal{R}}\|_2^2) \times \mathbb{P}[S_{\mathcal{R},1}^* = s_{\mathcal{R},1}^* \mid P_{\nu_{\mathcal{R}}}^\perp Y = P_{\nu_{\mathcal{R}}}^\perp y, \nu_{\mathcal{R}}^\top Y = t],$$

where $\nu_{\mathcal{R}}^\top \mu = \sqrt{n_{\mathcal{R}}} \mu_{\mathcal{R}}$ and $\phi(t; \mu, \gamma^2)$ denotes a normal density with mean parameter μ and variance γ^2 . In the above-stated conditional density, the second term represents the probability of observing the split $s_{\mathcal{R},1}^*$, conditional on the data variables. When combined with the naïve density of $\nu_{\mathcal{R}}^\top Y$, this yields the conditional density that provides valid inference

in the RRT. Computing this probability is central to the new inference approach, and due to the additive form of our randomization, we can easily derive an exact expression for it.

Below, we outline the main two steps for computing this probability, providing a formal derivation of its expression in the next section.

Step 1. First, observe that our event equals

$$\{S_{\mathcal{R},1}^* = s_{\mathcal{R},1}^*\} = \left\{ W_1(s_{\mathcal{R},1}^*) - W_1(s) \geq G(Y; P_1, s) - G(Y; P_1, s_{\mathcal{R},1}^*), \forall s \in \mathcal{X}_{\mathcal{R},1} \setminus \{s_{\mathcal{R},1}^*\} \right\}.$$

Step 2. Letting $y(t) = t \frac{\nu_{\mathcal{R}}}{\|\nu_{\mathcal{R}}\|_2^2} + P_{\nu_{\mathcal{R}}}^\perp y$ and taking probabilities of the two equivalent events in Step 1, we have

$$\begin{aligned} & \mathbb{P} \left[S_{\mathcal{R},1}^* = s_{\mathcal{R},1}^* \mid \nu_{\mathcal{R}}^\top Y = t, P_{\nu_{\mathcal{R}}}^\perp Y = P_{\nu_{\mathcal{R}}}^\perp y \right] \\ &= \mathbb{P} \left[W_1(s_{\mathcal{R},1}^*) - W_1(s) \geq G(Y; P_1, s) - G(Y; P_1, s_{\mathcal{R},1}^*), \right. \\ & \qquad \qquad \qquad \left. \forall s \in \mathcal{X}_{\mathcal{R},1} \setminus \{s_{\mathcal{R},1}^*\} \mid \nu_{\mathcal{R}}^\top Y = t, P_{\nu_{\mathcal{R}}}^\perp Y = P_{\nu_{\mathcal{R}}}^\perp y \right] \\ &= \mathbb{P} \left[W_1(s_{\mathcal{R},1}^*) - W_1(s) \geq G(y(t); P_1, s) - G(y(t); P_1, s_{\mathcal{R},1}^*), \forall s \in \mathcal{X}_{\mathcal{R},1} \setminus \{s_{\mathcal{R},1}^*\} \right]. \end{aligned}$$

The second equality uses the independence of the randomization variables from Y , and consequently, their independence from both $\nu_{\mathcal{R}}^\top Y$ and $P_{\nu_{\mathcal{R}}}^\perp Y$. Therefore, as long as we know the distribution of the differences $\{W_1(s_{\mathcal{R},1}^*) - W_1(s) : s \in \mathcal{X}_{\mathcal{R},1} \setminus \{s_{\mathcal{R},1}^*\}\}$, this probability is straightforward to compute. This is indeed the case, as we demonstrate in the next section. Due to the normal distribution of the randomization variables, this probability simplifies to an integral based on the Gaussian density of these randomization variables.

4 Exact pivot for inference

In this section, we derive the density for the conditional distribution in (2). We generalize the main ideas from the simple example in the previous section to account for the more complex selection of a series of splits and derive an exact pivot for inference in the TREE-model (1). We develop the inferential results for fixed-depth trees here, while extensions of our method and their theoretical guarantees for TREE-models fitted with adaptive stopping rules are provided in Appendix B.

To proceed, we fix some additional notation to track variables in the subtree leading to an observed terminal region \mathcal{R} . Let $\bar{P}_{\mathcal{R}} = \{P_{\mathcal{R},1} = \mathbb{R}^p, P_{\mathcal{R},2}, \dots, P_{\mathcal{R},L}\}$ denote the set of parent regions that were recursively split to obtain \mathcal{R} , i.e., the last split on $P_{\mathcal{R},L}$ results in the terminal region \mathcal{R} . Let $\chi_{\mathcal{R},l}$ denote the set of possible splits at the parent region $P_{\mathcal{R},l}$, where $|\chi_{\mathcal{R},l}| = d_l$, and let

$$\bar{S}_{\mathcal{R}} = \{S_{\mathcal{R},1}^*, S_{\mathcal{R},2}^*, \dots, S_{\mathcal{R},L}^*\}$$

be the series of L random splits made on this sequence of parent regions in $\bar{P}_{\mathcal{R}}$ leading to \mathcal{R} . As before, we let $\bar{s}_{\mathcal{R}} = \{s_{\mathcal{R},1}^*, s_{\mathcal{R},2}^*, \dots, s_{\mathcal{R},L}^*\}$ denote the observed values of these splits, i.e., for the specific TREE-model realized when $Y = y$, we observe $\{\bar{S}_{\mathcal{R}} = \bar{s}_{\mathcal{R}}\}$. Furthermore, we let $\bar{S}'_{\mathcal{R}} = \bar{S} \setminus \bar{S}_{\mathcal{R}}$ be the set of splits in the RRT that are not included in the subtree leading to \mathcal{R} , and we let $\bar{s}'_{\mathcal{R}}$ represent the observed values of these splits. Recall that at each split in this subtree, the RRT Algorithm 1 adds independent randomization variables to the gain function. We collect these randomization variables and denote them by $\bar{W}_{\mathcal{R}} = \{\bar{W}_{\mathcal{R},1}, \dots, \bar{W}_{\mathcal{R},L}\}$ where $\bar{W}_{\mathcal{R},l} = \{W_{\mathcal{R},l}(s), \forall s \in \chi_{\mathcal{R},l}\}$. For the reader's convenience, we summarize these notations in Table 1.

Variable/Object	Definition	Set/Vector
$\bar{P}_{\mathcal{R}}$	Parent regions of \mathcal{R}	$\{P_{\mathcal{R},1}, P_{\mathcal{R},2}, \dots, P_{\mathcal{R},L}\}$
$\bar{S}_{\mathcal{R}}$	Splits leading to \mathcal{R}	$\{S_{\mathcal{R},1}^*, S_{\mathcal{R},2}^*, \dots, S_{\mathcal{R},L}^*\}$
$\bar{W}_{\mathcal{R}}$	Randomization variables linked with $\bar{S}_{\mathcal{R}}$	$\{W_{\mathcal{R},1}, W_{\mathcal{R},2}, \dots, W_{\mathcal{R},L}\}$
$\bar{S}'_{\mathcal{R}}$	Splits not relevant to \mathcal{R}	$\bar{S} \setminus \bar{S}_{\mathcal{R}}$
$\bar{D}_{\mathcal{R}}$	Differences in gain functions linked with \mathcal{R}	$(D_{\mathcal{R},l} : l \in [L])$

Table 1: A list of notations for variables/objects in the subtree leading to an observed terminal region \mathcal{R}

4.1 Conditional density and an exact pivot

Our main result in this section, Theorem 4.2, provides the expression for an exact pivot, which is a function of the observed data $Y = y$ and our parameter of interest, $\mu_{\mathcal{R}}$. To state this result, we first establish a few useful results analyzing the conditional probability of the selection event given the observed data. These results ultimately lead to the conditional density for the distribution in (2).

Lemma 4.1 states that, to obtain the conditional density of interest, we only need to account for the selection of the splits in $\bar{S}_{\mathcal{R}}$, which form the subtree leading to \mathcal{R} .

Lemma 4.1. *For an observed terminal region $\mathcal{R} \in \bar{\mathcal{R}}$, it holds that*

$$\mathbb{P}[\bar{S} = \bar{s} \mid P_{\nu_{\mathcal{R}}}^{\perp} Y = P_{\nu_{\mathcal{R}}}^{\perp} y, \nu_{\mathcal{R}}^{\top} Y = t] \propto \mathbb{P}[\bar{S}_{\mathcal{R}} = \bar{s}_{\mathcal{R}} \mid P_{\nu_{\mathcal{R}}}^{\perp} Y = P_{\nu_{\mathcal{R}}}^{\perp} y, \nu_{\mathcal{R}}^{\top} Y = t],$$

when the probability on the left-hand side of the display is evaluated as a function of $\nu_{\mathcal{R}}^{\top} Y = t \in \mathbb{R}$.

Proposition 4.1 uses Lemma 4.1 to obtain the conditional density of interest.

Proposition 4.1. *The conditional density of $\nu_{\mathcal{R}}^{\top} Y \mid \{\bar{S} = \bar{s}, P_{\nu_{\mathcal{R}}}^{\perp} Y = P_{\nu_{\mathcal{R}}}^{\perp} y\}$, when evalu-*

ated at $\nu_{\mathcal{R}}^\top Y = t$, equals

$$\frac{\phi(t; \nu_{\mathcal{R}}^\top \mu, \sigma^2 \|\nu_{\mathcal{R}}\|_2^2) \times \mathbb{P}[\bar{S}_{\mathcal{R}} = \bar{s}_{\mathcal{R}} \mid P_{\nu_{\mathcal{R}}}^\perp Y = P_{\nu_{\mathcal{R}}}^\perp y, \nu_{\mathcal{R}}^\top Y = t]}{\int \phi(t'; \nu_{\mathcal{R}}^\top \mu, \sigma^2 \|\nu_{\mathcal{R}}\|_2^2) \times \mathbb{P}[\bar{S}_{\mathcal{R}} = \bar{s}_{\mathcal{R}} \mid P_{\nu_{\mathcal{R}}}^\perp Y = P_{\nu_{\mathcal{R}}}^\perp y, \nu_{\mathcal{R}}^\top Y = t'] dt'}.$$

Our next result, Proposition 4.2, provides an expression for the probability of the selected splits $\{\bar{S}_{\mathcal{R}} = \bar{s}_{\mathcal{R}}\}$, given data, as an explicit function of $(\nu_{\mathcal{R}}^\top Y, P_{\nu_{\mathcal{R}}}^\perp Y)$.

For the series of L selected splits $\bar{s}_{\mathcal{R}} = \{s_{\mathcal{R},1}^*, s_{\mathcal{R},2}^*, \dots, s_{\mathcal{R},L}^*\}$, define for each $l \in [L]$:

$$\begin{aligned} \beta_{s_{\mathcal{R},l}^*}(t, P_{\nu_{\mathcal{R}}}^\perp y) &= (G(y(t); P_{\mathcal{R},l}, s) - G(y(t); P_{\mathcal{R},l}, s_{\mathcal{R},l}^*) : s \in \chi_{\mathcal{R},l} \setminus \{s_{\mathcal{R},l}^*\}) \in \mathbb{R}^{d_l-1}, \\ \Omega_{\mathcal{R},l} &= \tau_{P_{\mathcal{R},l}}^2 (I_{d_l-1} + \mathbf{1}_{d_l-1} \mathbf{1}_{d_l-1}^\top) \in \mathbb{R}^{(d_l-1) \times (d_l-1)}, \end{aligned}$$

where $y(t) = t \frac{\nu}{\|\nu\|_2^2} + P_{\nu_{\mathcal{R}}}^\perp y$. The vector $\beta_{s_{\mathcal{R},l}^*}(t, P_{\nu_{\mathcal{R}}}^\perp y)$ collects the difference in the information gains between the optimal split $s_{\mathcal{R},l}^*$ and the losing splits $s \in \chi_{\mathcal{R},l} \setminus \{s_{\mathcal{R},l}^*\}$ that were not chosen. Then, we define

$$\Lambda_{s_{\mathcal{R},l}^*}(t, P_{\nu_{\mathcal{R}}}^\perp y) = \int_{\mathbb{R}_+^{d_l-1}} \phi(u; \beta_{s_{\mathcal{R},l}^*}(t, P_{\nu_{\mathcal{R}}}^\perp y), \Omega_{\mathcal{R},l}) du,$$

a function of $(t, P_{\nu_{\mathcal{R}}}^\perp y)$. Note that $\Lambda_{s_{\mathcal{R},l}^*}(t, P_{\nu_{\mathcal{R}}}^\perp y)$ is a Gaussian integral over the $(d_l - 1)$ -dimensional positive orthant.

Proposition 4.2. *Given an observed terminal region $\mathcal{R} \in \bar{\mathcal{R}}$, we have that*

$$\mathbb{P}[\bar{S}_{\mathcal{R}} = \bar{s}_{\mathcal{R}} \mid \nu_{\mathcal{R}}^\top Y = t, P_{\nu_{\mathcal{R}}}^\perp Y = P_{\nu_{\mathcal{R}}}^\perp y] = \prod_{l=1}^L \Lambda_{s_{\mathcal{R},l}^*}(t, P_{\nu_{\mathcal{R}}}^\perp y).$$

At last, let

$$\Lambda_{\bar{s}_{\mathcal{R}}}(t, P_{\nu_{\mathcal{R}}}^\perp y) = \prod_{l=1}^L \Lambda_{s_{\mathcal{R},l}^*}(t, P_{\nu_{\mathcal{R}}}^\perp y).$$

In Theorem 4.2, we present the final expression for an exact pivot, derived using the conditional density from Proposition 4.2.

Theorem 4.2. *Given data $Y = y$, let*

$$P(\nu_{\mathcal{R}}^{\top} y, P_{\nu_{\mathcal{R}}}^{\perp} y; \nu_{\mathcal{R}}^{\top} \mu) = \frac{\int_{-\infty}^{\nu_{\mathcal{R}}^{\top} y} \phi(t; \nu_{\mathcal{R}}^{\top} \mu, \sigma^2 \|\nu_{\mathcal{R}}\|_2^2) \Lambda_{\bar{s}_{\mathcal{R}}}(t, P_{\nu_{\mathcal{R}}}^{\perp} y) dt}{\int_{-\infty}^{+\infty} \phi(t; \nu_{\mathcal{R}}^{\top} \mu, \sigma^2 \|\nu_{\mathcal{R}}\|_2^2) \Lambda_{\bar{s}_{\mathcal{R}}}(t, P_{\nu_{\mathcal{R}}}^{\perp} y) dt}.$$

Then, it holds that

$$P(\nu_{\mathcal{R}}^{\top} Y, P_{\nu_{\mathcal{R}}}^{\perp} Y; \nu_{\mathcal{R}}^{\top} \mu) \mid \bar{S} = \bar{s} \sim \text{Unif}(0, 1).$$

The above result implies that for our observed data $Y = y$, the pivot for $\nu_{\mathcal{R}}^{\top} \mu$ equals $P(\nu_{\mathcal{R}}^{\top} y, P_{\nu_{\mathcal{R}}}^{\perp} y; \nu_{\mathcal{R}}^{\top} \mu)$. Referring back to (3), this pivot ensures valid inference in the RRT, achieving the nominal coverage rate while also controlling the FCR over the terminal regions fit with the RRT.

In Theorem 4.2, $\Lambda_{\bar{s}_{\mathcal{R}}}(t, P_{\nu_{\mathcal{R}}}^{\perp} y)$, for $t \in \mathbb{R}$, is the main ingredient for valid inference in the RRT. Multiplying this function with the naïve density of $\nu_{\mathcal{R}}^{\top} Y$ takes into account the data-dependent nature of \mathcal{R} , the terminal region linked to our parameter of interest $\mu_{\mathcal{R}}$.

The proposed pivot from Theorem 4.2 calculated under the null $\nu_{\mathcal{R}}^{\top} \mu = 0$ serves as valid p-value for testing. Moreover, to obtain confidence intervals for the selected target $\nu_{\mathcal{R}}^{\top} \mu$, we simply invert our pivot. For example, two-sided confidence intervals at level α are constructed as

$$(L_{\mathcal{R}}, U_{\mathcal{R}}) = \left\{ \nu_{\mathcal{R}}^{\top} \mu : P(\nu_{\mathcal{R}}^{\top} y, P_{\nu_{\mathcal{R}}}^{\perp} y; \nu_{\mathcal{R}}^{\top} \mu) \in \left[\frac{\alpha}{2}, 1 - \frac{\alpha}{2} \right] \right\}.$$

We note that the function $\Lambda_{\bar{s}_{\mathcal{R}}}(t, P_{\nu_{\mathcal{R}}}^{\perp} y)$, which restores the validity of inference, decou-

ples into L integrals, where L is the size of the subtree leading to \mathcal{R} . Each integral in this decomposition is a $(d_l - 1)$ -dimensional integral, where $d_l = |\chi_l|$. In the next section, we show that it is possible to reduce each such integral to a lower-dimensional integral, potentially as small as a one-dimensional integral, by applying careful additional conditioning. This leads to an efficient recipe to compute our pivot. As illustrated in Figures 1 and 2 in the introduction, even with this additional conditioning, we achieve considerably shorter intervals compared to the baseline conditional method in Neufeld et al. [2022] and alternatives based on data splitting like the UV method in Rasines and Young [2023].

4.2 Pivot with additional conditioning

Recall that we observed the selected series of splits: $\bar{s}_{\mathcal{R}} = \{s_{\mathcal{R},1}^*, s_{\mathcal{R},2}^*, \dots, s_{\mathcal{R},L}^*\}$. Following our earlier notations, for each $l \in [L]$, we define

$$D_{\mathcal{R},l}(s) = G(Y; P_{\mathcal{R},l}, s_{\mathcal{R},l}^*) + W_{\mathcal{R},l}(s_{\mathcal{R},l}^*) - G(Y; P_{\mathcal{R},l}, s) - W_{\mathcal{R},l}(s); \quad \forall s \in \chi_{\mathcal{R},l} \setminus \{s_{\mathcal{R},l}^*\}. \quad (4)$$

Let $D_{\mathcal{R},l} = (D_{\mathcal{R},l}(s) : s \in \chi_{\mathcal{R},l} \setminus \{s_{\mathcal{R},l}^*\})$ denote the $(d_l - 1)$ -dimensional vector which contains the difference between the randomized gains of the optimal split and the losing splits at the parent region $P_{\mathcal{R},l}$, and let $\bar{D}_{\mathcal{R}} = (D_{\mathcal{R},l} : l \in [L])$ collect these vectors across the L splits in the subtree leading to \mathcal{R} .

Lemma 4.3. *It holds that*

$$\{S_{\mathcal{R},l}^* = s_{\mathcal{R},l}^*\} = \{D_{\mathcal{R},l} \geq 0\}, \text{ for all } l \in [L], \text{ and } \{\bar{S}_{\mathcal{R}} = \bar{s}_{\mathcal{R}}\} = \{\bar{D}_{\mathcal{R}} \geq 0\}.$$

The proof of Lemma 4.3 is direct based on the definition of the randomized gains and the variable $D_{\mathcal{R},l}$ defined in (4) for $l \in [L]$.

We are now ready to present the additional conditioning we apply to obtain a pivot that is easy to compute. For each $l \in [L]$, assuming without loss of generality that no ties occur, let

$$0 < [D_{\mathcal{R},l}]_{(1)} < [D_{\mathcal{R},l}]_{(2)} < \cdots < [D_{\mathcal{R},l}]_{(d_l-1)}$$

denote the order statistics of the components of $D_{\mathcal{R},l}$ when arranged in ascending order. In the presence of ties, they are either resolved arbitrarily or handled using a prefixed rule that does not depend on the data. While $[D_{\mathcal{R},l}]_{(1)}$ represents the difference between the randomized gains of the optimal split $s_{\mathcal{R},l}^*$ and its closest competitor, $[D_{\mathcal{R},l}]_{(d_l-1)}$ captures the difference between the randomized gains of the optimal split from its farthest competitor.

For each $l \in [L]$, we propose to additionally condition on the indices of the $(d_l - 1 - r)$ largest values of $D_{\mathcal{R},l}$ along with their observed values, where $r \in \{1, 2, \dots, d_l - 1\}$. As we will see, this additional conditioning allows us to simplify the correction for the data-dependent selection of each split in the subtree, reducing it from a $(d_l - 1)$ -dimensional integral to an r -dimensional integral. Specifically, let $\mathcal{I}_{\mathcal{R},l}$ denote the indices of the $(d_l - 1 - r)$ largest values of $D_{\mathcal{R},l}$, and let $\mathcal{L}_{\mathcal{R},l} = \{1, 2, \dots, d_l - 1\} \setminus \mathcal{I}_{\mathcal{R},l}$, be the complement set of $\mathcal{I}_{\mathcal{R},l}$. Then, define

$$A_{\mathcal{R},l} = \{\mathcal{I}_{\mathcal{R},l}, (D_{\mathcal{R},l})_{k \in \mathcal{I}_{\mathcal{R},l}}\}$$

and let $\bar{A}_{\mathcal{R}}$ collect $A_{\mathcal{R},l}$ for $l \in [L]$. Consistent with our scheme for notations, we let $\bar{a}_{\mathcal{R}}$ denote the observed value of $\bar{A}_{\mathcal{R}}$.

It follows directly that $\{\bar{S}_{\mathcal{R}} = \bar{s}_{\mathcal{R}}, \bar{A}_{\mathcal{R}} = \bar{a}_{\mathcal{R}}\} \subseteq \{\bar{S}_{\mathcal{R}} = \bar{s}_{\mathcal{R}}\}$, and with this additional conditioning on the left-hand side, and following the argument in Lemma 4.1, we now need to compute the conditional density of

$$\nu_{\mathcal{R}}^{\top} Y \mid \{\bar{S}_{\mathcal{R}} = \bar{s}_{\mathcal{R}}, \bar{A}_{\mathcal{R}} = \bar{a}_{\mathcal{R}}, P_{\nu_{\mathcal{R}}}^{\perp} Y = P_{\nu_{\mathcal{R}}}^{\perp} y\}.$$

To compute this conditional density, we first note that the conditioning event can be described through simple constraints on the differences between the randomized gains defined in (4). This description is presented in Lemma 4.4.

Lemma 4.4. *Suppose that we observe $\{(D_{\mathcal{R},l})_{k'} = (\mathcal{D}_{\mathcal{R},l})_{k'}, \text{ for } k' \in \mathcal{I}_{\mathcal{R},l}\}$. We have that*

$$\{\bar{S}_{\mathcal{R}} = \bar{s}_{\mathcal{R}}, \bar{A}_{\mathcal{R}} = \bar{a}_{\mathcal{R}}\} = \bigcap_{l \in [L]} \left\{ \begin{aligned} &0 < (D_{\mathcal{R},l})_k < [D_{\mathcal{R},l}]_{(r+1)} \text{ for all } k \in \mathcal{L}_{\mathcal{R},l}, \\ &(D_{\mathcal{R},l})_{k'} = (\mathcal{D}_{\mathcal{R},l})_{k'} \text{ for all } k' \in \mathcal{I}_{\mathcal{R},l}. \end{aligned} \right\}.$$

We then compute a pivot after the additional conditioning, as presented in Theorem 4.5. To state this pivot, let $\mathcal{D}_{\mathcal{R},l}^{(r)} = \{(\mathcal{D}_{\mathcal{R},l})_{k'} : k' \in \mathcal{I}_{\mathcal{R},l}\}$ and let $\mathcal{D}_{\mathcal{R}}^{(r)} = \{\mathcal{D}_{\mathcal{R},l}^{(r)} : l \in [L]\}$. Define the vectors:

$$\begin{aligned} \beta_{\mathcal{R},l}^1(t, P_{\nu_{\mathcal{R}}}^{\perp} y) &= (G(y(t); P_{\mathcal{R},l}, s_{\mathcal{R},l}^*) - G(y(t); P_{\mathcal{R},l}, s_k) : k \in \mathcal{L}_{\mathcal{R},l}) \in \mathbb{R}^r \\ \beta_{\mathcal{R},l}^2(t, P_{\nu_{\mathcal{R}}}^{\perp} y) &= (G(y(t); P_{\mathcal{R},l}, s_{\mathcal{R},l}^*) - G(y(t), y); P_{\mathcal{R},l}, s_k) : k \in \mathcal{I}_{\mathcal{R},l}) \in \mathbb{R}^{d_l - r - 1}. \end{aligned}$$

Let the matrix $\Omega_{\mathcal{R},l}$ be partitioned into the $r \times r$ and $(d_l - r - 1) \times (d_l - r - 1)$ -dimensional matrices, where the first r indices correspond to the set $\mathcal{L}_{\mathcal{R},l}$ and the last $(d_l - r - 1)$ indices

correspond to the set $\mathcal{I}_{\mathcal{R},l}$, as follows: $\Omega_{\mathcal{R},l} = \begin{bmatrix} \Omega_{\mathcal{R},l}^{1,1} & \Omega_{\mathcal{R},l}^{1,2} \\ \Omega_{\mathcal{R},l}^{2,1} & \Omega_{\mathcal{R},l}^{2,2} \end{bmatrix}$.

At last, suppose that

$$\begin{aligned} \beta_{s_{\mathcal{R},l}^*, a_{\mathcal{R},l}}(t, P_{\nu_{\mathcal{R}}}^{\perp} y) &= \beta_{\mathcal{R},l}^1(t, P_{\nu_{\mathcal{R}}}^{\perp} y) + \Omega_{\mathcal{R},l}^{1,2} (\Omega_{\mathcal{R},l}^{2,2})^{-1} \left(\mathcal{D}_{\mathcal{R},l}^{(r)} - \beta_{\mathcal{R},l}^2(t, P_{\nu_{\mathcal{R}}}^{\perp} y) \right) \in \mathbb{R}^r \\ \Sigma_{\mathcal{R},l} &= \Omega_{\mathcal{R},l}^{1,1} - \Omega_{\mathcal{R},l}^{1,2} (\Omega_{\mathcal{R},l}^{2,2})^{-1} \Omega_{\mathcal{R},l}^{2,1} \in \mathbb{R}^{r \times r}. \end{aligned}$$

Then, for $H_{\mathcal{R},l}^{(r)} = \{u \in \mathbb{R}^r : 0 < u_k < [D_{\mathcal{R},l}]_{(r+1)} \text{ for } k \in [r]\}$, define

$$\Gamma_{s_{\mathcal{R},l}^*, a_{\mathcal{R},l}}(t, P_{\nu_{\mathcal{R}}}^\perp y, \mathcal{D}_{\mathcal{R},l}^{(r)}) = \phi\left(\mathcal{D}_{\mathcal{R},l}^{(r)}; \beta_{\mathcal{R},l}^2(t, P_{\nu_{\mathcal{R}}}^\perp y), \Omega_{\mathcal{R},l}^{2,2}\right) \times \int_{H_{\mathcal{R},l}^{(r)}} \phi\left(u; \beta_{s_{\mathcal{R},l}^*, a_{\mathcal{R},l}}(t, P_{\nu_{\mathcal{R}}}^\perp y), \Sigma_{\mathcal{R},l}\right) du,$$

and let

$$\Gamma_{\bar{s}_{\mathcal{R}}, \bar{a}_{\mathcal{R}}}(t, P_{\nu_{\mathcal{R}}}^\perp y, \mathcal{D}_{\mathcal{R}}^{(r)}) = \prod_{l=1}^L \Gamma_{s_{\mathcal{R},l}^*, a_{\mathcal{R},l}}(t, P_{\nu_{\mathcal{R}}}^\perp y, \mathcal{D}_{\mathcal{R},l}^{(r)}).$$

Theorem 4.5. *Given data $Y = y$, let*

$$\tilde{P}(\nu_{\mathcal{R}}^\top y, P_{\nu_{\mathcal{R}}}^\perp y; \nu_{\mathcal{R}}^\top \mu) = \frac{\int_{-\infty}^{\nu_{\mathcal{R}}^\top y} \phi(t; \nu_{\mathcal{R}}^\top \mu, \sigma^2 \|\nu_{\mathcal{R}}\|_2^2) \Gamma_{\bar{s}_{\mathcal{R}}, \bar{a}_{\mathcal{R}}}(t, P_{\nu_{\mathcal{R}}}^\perp y, \mathcal{D}_{\mathcal{R}}^{(r)}) dt}{\int_{-\infty}^{+\infty} \phi(t; \nu_{\mathcal{R}}^\top \mu, \sigma^2 \|\nu_{\mathcal{R}}\|_2^2) \Gamma_{\bar{s}_{\mathcal{R}}, \bar{a}_{\mathcal{R}}}(t, P_{\nu_{\mathcal{R}}}^\perp y, \mathcal{D}_{\mathcal{R}}^{(r)}) dt}.$$

Then, it holds that

$$\tilde{P}(\nu_{\mathcal{R}}^\top Y, P_{\nu_{\mathcal{R}}}^\perp Y; \nu_{\mathcal{R}}^\top \mu) \mid \bar{S} = \bar{s} \sim \text{Unif}(0, 1).$$

The proof of Theorem 4.5 is provided in Appendix A.

When $r = 1$, the correction function $\Gamma_{\bar{s}_{\mathcal{R}}, \bar{a}_{\mathcal{R}}}(t, P_{\nu_{\mathcal{R}}}^\perp y, \mathcal{D}_{\mathcal{R}}^{(r)})$, used to account for the selection in each split of the relevant sub-tree, reduces to computing L one-dimensional integrals in our exact pivot.

5 Simulation

Here we present a simulation study to demonstrate the suitability of our proposed method and compare to existing approaches. We generate the data in a similar fashion to the simulation studies in Neufeld et al. [2022], where $X \in \mathbb{R}^{n \times p}$ with $n = 200$, $X_{ij} \stackrel{i.i.d.}{\sim} N(0, 1)$, and $Y = \mu + \epsilon$. The vector μ given by $\mu_i = b \times [1_{(x_{i,1} \leq 0)} \times \{1 + a1_{(x_{i,2} > 0)} + 1_{(x_{i,3} \times x_{i,2} > 0)}\}]$ defines a three-level tree where $a = 1$, $b = 2$ determine the signal strength. The noise $\epsilon_i \stackrel{i.i.d.}{\sim} D$ are independently drawn random noise. For each fitting method, we set the

maximum depth of the final tree as 3, the minimum number of samples in a node to be split further as 50, the minimum size of terminal nodes as 20, and leave the grown tree unpruned after the stopping criterion is met.

After fitting the trees and constructing confidence intervals for terminal regions using our proposed method along with the three baseline methods described above, we consider the following evaluation metrics for comparison:

1. **Coverage rate:** In each round of simulation, for a regression tree $TREE$ fitted with terminal nodes \bar{R} , we compute the coverage rate as $|\{R \in \bar{R} : \nu_R^\top \mu \in \text{CI}_R\}|/|\bar{R}|$
2. **Average CI length:** To measure the inferential power of the tests, we report the average length of the confidence intervals $\text{CI}_R = (L_R, U_R)$, i.e., $\{\sum_{R \in \bar{R}} (U_R - L_R)\}/|\bar{R}|$.
3. **Test MSE:** To examine the model fitting quality of different methods, we generate new test data $Y^{\text{test}} = \mu + \epsilon^{\text{test}}$, where $\epsilon_i^{\text{test}} \stackrel{i.i.d.}{\sim} D$ is a new vector of independently drawn random noise. Then, for each sample we compute its predicted response value $\hat{\mu}(X_i) = \sum_{R \in \bar{R}} \bar{Y}_R 1_{(X_i \in R)}$, and the test MSE, i.e., $\sum_{i=1}^n (Y_i^{\text{test}} - \hat{\mu}(X_i))^2/n$.

5.1 Results under varying Gaussian noise scales

To evaluate the performance of the proposed method compared to the baseline methods under varying signal strengths, we fix $p = 10$ and vary the noise distribution $D = \mathcal{N}(0, \sigma_G^2)$ for $\sigma_G \in \{1, 2, 5, 10\}$ and employ our proposed method with the randomization sd parameter $\tau_P = \tau = c * \sigma_G$ for $c = 1$, i.e., $\text{RRT}(1)$. We compare the empirical performance on the same simulated dataset over 500 simulations of our proposal with that of the Tree-values method and the UV method described in Section 1. The resulting coverage rates, average confidence interval lengths, and test MSE are presented in Figure 3.

While all three methods approximately achieve the targeted coverage rate of 90%, the proposed method produces confidence intervals that are shorter than Tree-values intervals by orders of magnitude. Additionally, our intervals are generally shorter than UV intervals across all settings, except in the case of the signal setting with the highest noise. Since there is almost no residual information in the data used for selection that could have been utilized for inference, our intervals are only comparable to the UV intervals in this setting. Furthermore, the proposed method results in favorable test MSE performance compared to the two baseline methods. See Appendix C for an additional comparison that demonstrates these conclusions are similar under misspecification of the error distribution.

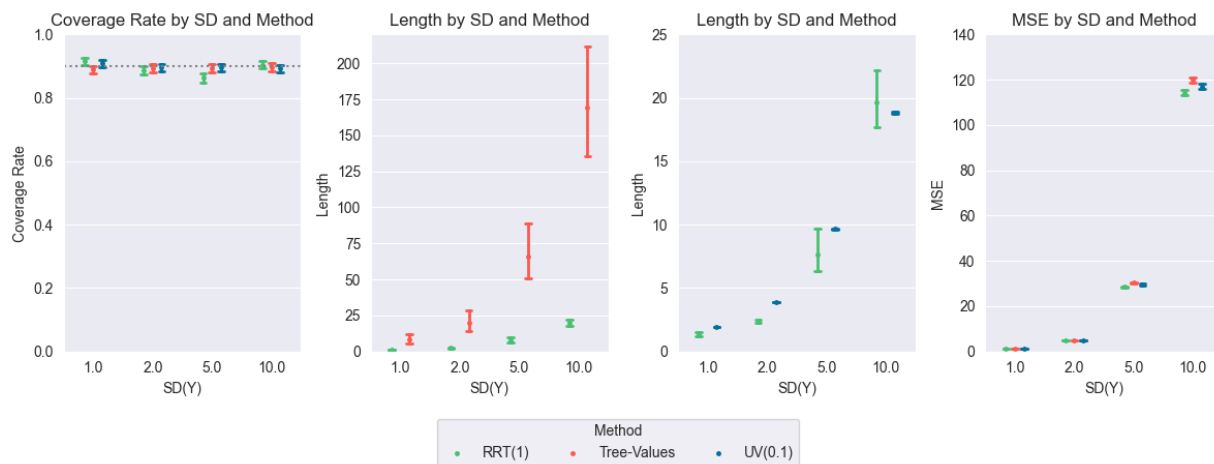


Figure 3: Coverage rate, average CI length, and prediction MSE of RRT(1), Tree-Values, and the UV method for $\sigma_G^2 \in \{1, 2, 5, 10\}$ and Gaussian noise; The dotted line is plotted at 0.9 in the coverage plot

5.2 Results under varying dimensions

We generate data similar to the previous simulation. To evaluate the performance of the proposed method compared to the baseline methods under dense/sparse signals, we vary the number of covariates $p \in \{5, 10, 20\}$, corresponding to 2, 7, 17, noise variables, respectively. Similarly, in Figure 4, while all three methods approximately achieve the targeted coverage

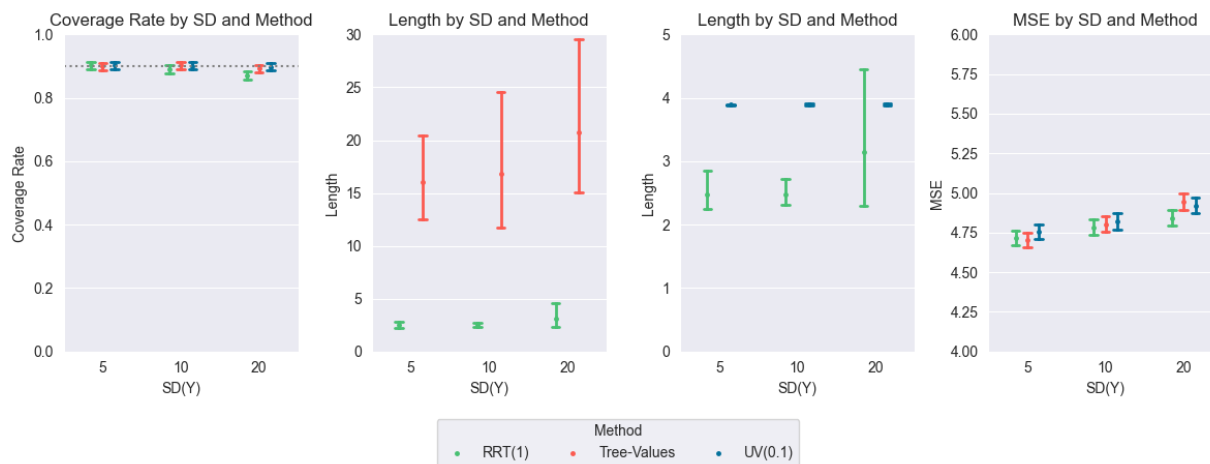


Figure 4: Coverage rate, average CI length, and prediction MSE of RRT(1), UV method, and Tree-Values for $p \in \{5, 10, 20\}$; The dotted line is plotted at 0.9 in the coverage plot rate of 90%, the proposed method yields intervals that are shorter than Tree-values intervals and the UV intervals on average. Importantly, our method does not compromise predictive performance to inferential power, as reflected in the test MSE comparison.

6 Case study: PROMPT

The *PROviding Mental health Precision Treatment (PROMPT) Precision Health Study* is a 12-month mobile health intervention trial focused on reducing the burden of depression by augmenting standard mental health care using mobile health technologies to support patients on the wait list for traditional care. Adult patients (age 18+) who have a scheduled mental health intake appointments at either Michigan Medicine Outpatient Psychiatry or University Health Service clinics were eligible for participation. Recruited patients entered study at least 2 weeks prior to their initial clinic appointment. Participants were asked to complete surveys throughout the study, including an initial intake survey and a 6-week follow-up survey. Each study participant received a Fitbit to wear daily for the duration of their time in the study.

Here, we study the predictive power of the initial intake survey and wearable device data collected over the first study month on a measure of depression severity reported at the 6-week follow-up survey known as the Patient Health Questionnaire 9 (PHQ-9). To predict the PHQ-9, we compute summary statistics, such as means and standard deviations, of 15 daily variables. Additionally, we aggregated individual patient responses to each of 9 different intake surveys, including the intake PHQ-9 and the intake General Anxiety Disorder (GAD-7) to create severity scores for each of these 9 surveys. After dropping variables with high missing rates (20%), such as variables requiring consistent user input, we include 12 (summarized) sensor variables and 9 intake survey variables in the tree model. The final list of variables is included in Table 4 from Appendix D. Our final dataset consists of $N = 500$ patients with 21 sensor and intake survey variables as predictors, and the PHQ-9 severity score as the response.

Subsampling & methods comparison. To compare the predictive and inferential power of the proposed RRT method with existing methods, we include Tree-values and the UV method as baseline methods. For predictive power comparisons, we first split the dataset into a train set with $N_{\text{train}} = 300$ samples and a test set with $N_{\text{test}} = 200$ samples. Furthermore, for a comparison of all methods in a more realistic scientific setting with incoming data streams, we further subsample the train data with 50% and 75% samples of the full training set, with $N_{\text{train}50\%} = 150$ and $N_{\text{train}75\%} = 225$ samples, respectively.

All three methods are first fitted on the three datasets with 50%, 75%, and 100% samples of the full data, with the maximum depth of the final tree as 4, the minimum number of samples in a node to be split further as 50, the minimum size of terminal nodes as 20, and leave the grown tree unpruned after the stopping criterion is met. We set $\tau_P = \tau = c * \hat{\sigma}$ for $c = 1$ for the RRT method, i.e., RRT(1) and $\gamma = 0.1$ for the UV

method, i.e., UV(0.1), where $\hat{\sigma}$ is the sample estimate for σ . The confidence intervals for the means of the terminal regions are computed after model fitting. Finally, the predictive performance of fitted models is evaluated on the holdout testing set, measured by the MSE.

Empirical results and findings. Table 2 summarizes the average lengths of confidence intervals for the mean of terminal nodes given by the three different methods under different subsampling proportions of the training dataset. Consistent with the observations in the simulation study, the proposed method produces the shortest intervals on average. In particular, the Tree-values method can produce much longer confidence intervals given the small sample sizes.

Proportion	50%	75%	100%
Tree-Values	12.588	80.500	20.474
UV	10.745	12.510	12.017
Proposed	9.105	12.436	9.330

Table 2: Average CI lengths for different proportions of training data

Proportion	50%	75%	100%
Tree-Values	29.812	29.204	29.649
UV	30.685	30.545	28.872
Proposed	28.809	28.159	27.543

Table 3: Test MSE for different proportions of training data

Second, Table 3 shows all three methods have comparable MSE when validated on the test set. This again echoes the observations in the simulation study and confirmed that the proposed randomized procedure does not compromise the predictive power for a more powerful inference.

Finally, the tree structure fitted on the full training set using RRT is provided in Figure 5. The intervals shown in the terminal nodes are the confidence intervals for the corresponding node means.

Existing literature uses the following criteria to impute depression severity levels based on PHQ scores: minimal (0–4), mild (5–9), moderate (10–14), moderately severe (15–19), and severe (20–27), Kroenke et al. [2001]. Based on the confidence intervals generated

for the terminal nodes, we estimated that patients with high intake PHQ scores ($\text{PHQ_B} > 25$) fall into the range of mild-severe depression levels (node 9). For patients whose intake PHQ scores are within the range of 18 to 25, those having higher basal metabolic rates ($\text{CaloriesBMR} \leq 1325.46$) are estimated to have moderate-severe depression, while those having lower basal metabolic rates are estimated to have only mild-moderately severe depression (node 7 & 8). In contrast, for patients with lower intake PHQ scores ($\text{PHQ_B} \leq 18$), the fitted tree uses other intake survey scores to predict the 6-week PHQ score. For these patients, none of the corresponding terminal nodes (nodes 1-6) falls in the range of severe 6-week depression based on the confidence intervals generated for these nodes.

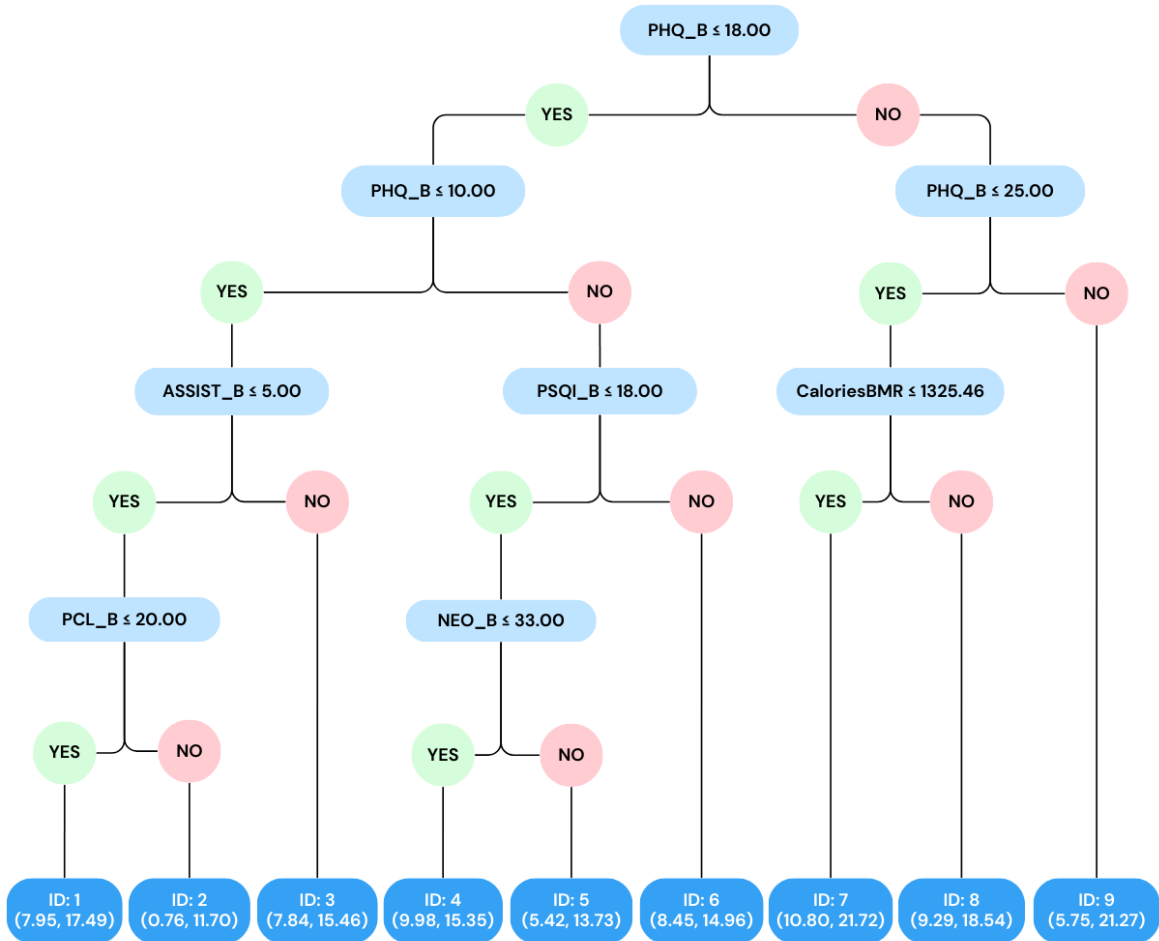


Figure 5: Fitted RRT on the full PROMPT training set

7 Conclusion

In this paper, we introduce a novel conditional selective inference framework that converts regression trees—one of the common tools in a statistician’s toolkit for non-linear regression—into a method capable of addressing inferential questions in the models they fit. Our method, called Randomized Regression Trees (RRT), adds external randomization to the gain functions underlying the splitting rules. We use this external randomization to derive an exact, closed-form pivot, enabling inference on the full dataset while accounting for the data-dependent nature of the model. The added randomization serves as a flexible lever to balance the tradeoff between the predictive accuracy of the model fit and the inferential reliability and power of the fitted model. Though, determining this tradeoff in practice can be challenging, as is often the case with data-splitting methods. In our work, we demonstrate that with a small amount of randomization, RRT matches the predictive accuracy of the model fit on the full dataset while delivering substantially shorter confidence intervals compared to those based solely on the held-out dataset, as done with data-splitting.

An immediate extension of our approach is to develop inference methods for classification trees. Given that randomization has been successfully employed in prior work, such as Panigrahi [2023], to enable valid asymptotic selective inference for data-dependent parameters, we plan to extend our methodology to classification problems in future research. A new form of randomization is used in our work to attach inference to regression trees. Naturally, this randomization can also be applied to construct a new type of random forests, by averaging over many randomized trees. We hope to investigate the potential of external randomization techniques to improve the interpretability of ensemble models, such as random forests.

8 Acknowledgements

We acknowledge the PROviding Mental health Precision Treatment (PROMPT) Precision Health Study at the University of Michigan for granting us access to the PROMPT data. Details of the study can be found at <https://um-prompt.wixsite.com/prompt>.

References

- Susan Athey and Guido Imbens. Recursive partitioning for heterogeneous causal effects. *Proceedings of the National Academy of Sciences*, 113(27):7353–7360, 2016. doi: 10.1073/pnas.1510489113. URL <https://www.pnas.org/doi/abs/10.1073/pnas.1510489113>.
- Soham Bakshi, Walter Dempsey, and Snigdha Panigrahi. Selective inference for time-varying effect moderation, 2024. URL <https://arxiv.org/abs/2411.15908>.
- Yoav Benjamini and Daniel Yekutieli. False discovery rate-adjusted multiple confidence intervals for selected parameters. *Journal of the American Statistical Association*, 100(469):71–81, 2005.
- L. Breiman, J. Friedman, C.J. Stone, and R.A. Olshen. *Classification and Regression Trees*. Taylor & Francis, 1984. ISBN 9780412048418. URL <https://books.google.com/books?id=JwQx-W0mSyQC>.
- Ali Charkhi and Gerda Claeskens. Asymptotic post-selection inference for the akaike information criterion. *Biometrika*, 105(3):645–664, 2018.
- Bradley Efron. Prediction, estimation, and attribution. *International Statistical Review*, 88(S1):S28–S59, 2020. doi: <https://doi.org/10.1111/insr.12409>. URL <https://onlinelibrary.wiley.com/doi/abs/10.1111/insr.12409>.

- Lucy L Gao, Jacob Bien, and Daniela Witten. Selective inference for hierarchical clustering. *Journal of the American Statistical Association*, 119(545):332–342, 2024.
- Jelle J Goeman and Aldo Solari. On selection and conditioning in multiple testing and selective inference. *Biometrika*, 111(2):393–416, 2024.
- Yiling Huang, Snigdha Panigrahi, and Walter Dempsey. Selective inference for sparse graphs via neighborhood selection. *arXiv preprint arXiv:2312.16734*, 2023a.
- Yiling Huang, Sarah Pirenne, Snigdha Panigrahi, and Gerda Claeskens. Selective inference using randomized group lasso estimators for general models. *arXiv preprint arXiv:2306.13829*, 2023b.
- Danijel Kivaranovic and Hannes Leeb. On the length of post-model-selection confidence intervals conditional on polyhedral constraints. *Journal of the American Statistical Association*, 116(534):845–857, 2021. doi: 10.1080/01621459.2020.1732989. URL <https://doi.org/10.1080/01621459.2020.1732989>.
- Kurt Kroenke, Robert L Spitzer, and Janet BW Williams. The phq-9: validity of a brief depression severity measure. *Journal of general internal medicine*, 16(9):606–613, 2001.
- Jason D. Lee, Dennis L. Sun, Yuekai Sun, and Jonathan E. Taylor. Exact post-selection inference, with application to the lasso. *The Annals of Statistics*, 44(3), June 2016. ISSN 0090-5364. doi: 10.1214/15-aos1371. URL <http://dx.doi.org/10.1214/15-AOS1371>.
- James Leiner, Boyan Duan, Larry Wasserman, and Aaditya Ramdas. Data fission: splitting a single data point. *Journal of the American Statistical Association*, pages 1–12, 2023.
- Sifan Liu. An exact sampler for inference after polyhedral model selection. *arXiv preprint arXiv:2308.10346*, 2023.

Wei-Yin Loh, Michael Man, and Shuaicheng Wang. Subgroups from regression trees with adjustment for prognostic effects and postselection inference. *Stat Med*, 38(4):545–557, April 2018.

Anna C Neufeld, Lucy L Gao, and Daniela M Witten. Tree-values: selective inference for regression trees. *Journal of Machine Learning Research*, 23(305):1–43, 2022.

Snigdha Panigrahi. Carving model-free inference. *The Annals of Statistics*, 51(6):2318–2341, 2023.

Snigdha Panigrahi and Jonathan Taylor. Approximate selective inference via maximum likelihood. *Journal of the American Statistical Association*, 118(544):2810–2820, 2023. doi: 10.1080/01621459.2022.2081575. URL <https://doi.org/10.1080/01621459.2022.2081575>.

Snigdha Panigrahi, Peter W MacDonald, and Daniel Kessler. Approximate post-selective inference for regression with the group lasso. *Journal of machine learning research*, 24(79):1–49, 2023.

Snigdha Panigrahi, Kevin Fry, and Jonathan Taylor. Exact selective inference with randomization. *Biometrika*, 111(4):1109–1127, 04 2024. ISSN 1464-3510. doi: 10.1093/biomet/asae019. URL <https://doi.org/10.1093/biomet/asae019>.

Ronan Perry, Snigdha Panigrahi, Jacob Bien, and Daniela Witten. Inference on the proportion of variance explained in principal component analysis. *arXiv preprint arXiv:2402.16725*, 2024.

Sarah Pirenne and Gerda Claeskens. Parametric programming-based approximate selective

- inference for adaptive lasso, adaptive elastic net and group lasso. *Journal of Statistical Computation and Simulation*, pages 1–24, 2024.
- D García Rasines and G Alastair Young. Splitting strategies for post-selection inference. *Biometrika*, 110(3):597–614, 2023.
- Xiaoying Tian and Jonathan Taylor. Selective inference with a randomized response. *The Annals of Statistics*, 46(2):679–710, 2018.
- Kurt Hornik Torsten Hothorn and Achim Zeileis. Unbiased recursive partitioning: A conditional inference framework. *Journal of Computational and Graphical Statistics*, 15(3):651–674, 2006. doi: 10.1198/106186006X133933. URL <https://doi.org/10.1198/106186006X133933>.
- Stefan Wager and Guenther Walther. Adaptive concentration of regression trees, with application to random forests, 2016. URL <https://arxiv.org/abs/1503.06388>.
- Qingyuan Zhao, Dylan S. Small, and Ashkan Ertefaie. Selective inference for effect modification via the lasso. *Journal of the Royal Statistical Society Series B: Statistical Methodology*, 84(2):382–413, 12 2021. ISSN 1369-7412. doi: 10.1111/rssb.12483. URL <https://doi.org/10.1111/rssb.12483>.

Appendices

A Proofs of main results in Section 4

Proof of Lemma 4.1. Observe that

$$\begin{aligned}
 & \mathbb{P} [\bar{S} = \bar{s} \mid P_{\nu_{\mathcal{R}}}^{\perp} Y = P_{\nu_{\mathcal{R}}}^{\perp} y, \nu_{\mathcal{R}}^{\top} Y = t] \\
 &= \mathbb{P} [\bar{S}_{\mathcal{R}} = \bar{s}_{\mathcal{R}}, \bar{S}'_{\mathcal{R}} = \bar{s}'_{\mathcal{R}} \mid P_{\nu_{\mathcal{R}}}^{\perp} Y = P_{\nu_{\mathcal{R}}}^{\perp} y, \nu_{\mathcal{R}}^{\top} Y = t] \\
 &= \underbrace{\mathbb{P} [\bar{S}_{\mathcal{R}} = \bar{s}_{\mathcal{R}} \mid \bar{S}'_{\mathcal{R}} = \bar{s}'_{\mathcal{R}}, P_{\nu_{\mathcal{R}}}^{\perp} Y = P_{\nu_{\mathcal{R}}}^{\perp} y, \nu_{\mathcal{R}}^{\top} Y = t]}_{(P1)} \underbrace{\mathbb{P} [\bar{S}'_{\mathcal{R}} = \bar{s}'_{\mathcal{R}} \mid P_{\nu_{\mathcal{R}}}^{\perp} Y = P_{\nu_{\mathcal{R}}}^{\perp} y, \nu_{\mathcal{R}}^{\top} Y = t]}_{(P2)}.
 \end{aligned}$$

To prove our claim, we show the following

$$(P1) = \mathbb{P} [\bar{S}_{\mathcal{R}} = \bar{s}_{\mathcal{R}} \mid P_{\nu_{\mathcal{R}}}^{\perp} Y = P_{\nu_{\mathcal{R}}}^{\perp} y, \nu_{\mathcal{R}}^{\top} Y = t],$$

$$(P2) = \mathbb{P} [\bar{S}'_{\mathcal{R}} = \bar{s}'_{\mathcal{R}} \mid P_{\nu_{\mathcal{R}}}^{\perp} Y = P_{\nu_{\mathcal{R}}}^{\perp} y].$$

This leads us to conclude that:

$$\mathbb{P} [\bar{S} = \bar{s} \mid P_{\nu_{\mathcal{R}}}^{\perp} Y = P_{\nu_{\mathcal{R}}}^{\perp} y, \nu_{\mathcal{R}}^{\top} Y = t] \propto \mathbb{P} [\bar{S}_{\mathcal{R}} = \bar{s}_{\mathcal{R}} \mid P_{\nu_{\mathcal{R}}}^{\perp} Y = P_{\nu_{\mathcal{R}}}^{\perp} y, \nu_{\mathcal{R}}^{\top} Y = t].$$

Firstly, note that any split $S_j^* \in \bar{S}$ made on $P_j \in \bar{P}$ is a function of $(\{Y_i : X_i \in P_j\}, \bar{W}_j)$, which are the observations whose covariates fall within P_j and the independent randomization variable that was added to the gain functions while selecting this split.

Define

$$Y(t) = t \frac{\nu}{\|\nu\|_2^2} + P_{\nu_{\mathcal{R}}}^{\perp} Y.$$

Then for a pair of splits $(S_j^*, S_{j'}^*) \in \bar{S} \times \bar{S}$, such that $j \neq j'$, we have that $S_j^* \perp\!\!\!\perp S_{j'}^* \mid Y(t) =$

$y(t)$, since $\overline{W}_j \perp\!\!\!\perp \overline{W}_{j'}$ for splits made on distinct parent regions. As a result, we also have that

$$S_j^* \perp\!\!\!\perp S_{j'}^* \mid \{P_{\nu_{\mathcal{R}}}^\perp Y = P_{\nu_{\mathcal{R}}}^\perp y, \nu_{\mathcal{R}}^\top Y = t\},$$

and that $\overline{S}_{\mathcal{R}} \perp\!\!\!\perp \overline{S}'_{\mathcal{R}} \mid \{P_{\nu_{\mathcal{R}}}^\perp Y = P_{\nu_{\mathcal{R}}}^\perp y, \nu_{\mathcal{R}}^\top Y = t\}$. This proves the claim about (P1).

Now, for any $S_j^* \in \overline{S}'_{\mathcal{R}}$ made on $P_j \in \overline{P}$, we have that $\mathcal{R} \cap P_j = \emptyset$. For such a P_j with a disjoint intersection with \mathcal{R} , given that $\overline{W} \perp\!\!\!\perp Y$ and that $\{Y_i : X_i \in P_j\} \perp\!\!\!\perp \nu_{\mathcal{R}}^\top Y$, we have

$$S_j^* \perp\!\!\!\perp \nu_{\mathcal{R}}^\top Y.$$

This proves our claim about (P2) immediately. \square

Proof of Proposition 4.1. The conditional density of $\nu_{\mathcal{R}}^\top Y \mid \{\overline{S} = \overline{s}, P_{\nu_{\mathcal{R}}}^\perp Y = P_{\nu_{\mathcal{R}}}^\perp y\}$ at t is proportional to

$$\phi(t; \nu_{\mathcal{R}}^\top \mu, \sigma^2 \|\nu_{\mathcal{R}}\|_2^2) \times \mathbb{P}[\overline{S}(Y, \overline{W}) = \overline{s} \mid \nu_{\mathcal{R}}^\top Y = t, P_{\nu_{\mathcal{R}}}^\perp Y = P_{\nu_{\mathcal{R}}}^\perp y],$$

due to the independence between $\nu_{\mathcal{R}}^\top Y$ and $P_{\nu_{\mathcal{R}}}^\perp Y$. Using the conclusion in Lemma 4.1, we further note that this density is proportional to

$$\phi(t; \nu_{\mathcal{R}}^\top \mu, \sigma^2 \|\nu_{\mathcal{R}}\|_2^2) \times \mathbb{P}[\overline{S}_{\mathcal{R}} = \overline{s}_{\mathcal{R}} \mid P_{\nu_{\mathcal{R}}}^\perp Y = P_{\nu_{\mathcal{R}}}^\perp y, \nu_{\mathcal{R}}^\top Y = t],$$

since

$$\mathbb{P}[\overline{S} = \overline{s} \mid \nu_{\mathcal{R}}^\top Y = t, P_{\nu_{\mathcal{R}}}^\perp Y = P_{\nu_{\mathcal{R}}}^\perp y] \propto \mathbb{P}[\overline{S}_{\mathcal{R}} = \overline{s}_{\mathcal{R}} \mid \nu_{\mathcal{R}}^\top Y = t, P_{\nu_{\mathcal{R}}}^\perp Y = P_{\nu_{\mathcal{R}}}^\perp y].$$

This leads to the claimed conditional density. \square

Proof of Proposition 4.2. We begin by noting that

$$\begin{aligned}
\{\bar{S}_{\mathcal{R}} = \bar{s}_{\mathcal{R}}\} &= \{S_{\mathcal{R},1}^* = s_{\mathcal{R},1}^*, S_{\mathcal{R},2}^* = s_{\mathcal{R},2}^*, \dots, S_{\mathcal{R},L}^* = s_{\mathcal{R},L}^*\} \\
&= \bigcap_{l=1}^L \{S_{\mathcal{R},l}^* = s_{\mathcal{R},l}^*\} \\
&= \bigcap_{l=1}^L \left\{ G(Y; P_{\mathcal{R},l}, s_{\mathcal{R},l}^*) - G(Y; P_{\mathcal{R},l}, s) + W_{\mathcal{R},l}(s_{\mathcal{R},l}^*) - W_{\mathcal{R},l}(s) \geq 0, \right. \\
&\qquad\qquad\qquad \left. \forall s \in \chi_{\mathcal{R},l}^* \setminus \{s_{\mathcal{R},l}^*\} \right\} \\
&= \bigcap_{l=1}^L \left\{ W_{\mathcal{R},l}(s_{\mathcal{R},l}^*) - W_{\mathcal{R},l}(s) \geq G(Y; P_{\mathcal{R},l}, s) - G(Y; P_{\mathcal{R},l}, s_{\mathcal{R},l}^*), \right. \\
&\qquad\qquad\qquad \left. \forall s \in \chi_{\mathcal{R},l}^* \setminus \{s_{\mathcal{R},l}^*\} \right\}.
\end{aligned} \tag{5}$$

Computing the probability of this event, it holds that

$$\begin{aligned}
&\mathbb{P}[\bar{S}_{\mathcal{R}} = \bar{s}_{\mathcal{R}} \mid \nu_{\mathcal{R}}^{\top} Y = t, P_{\nu_{\mathcal{R}}}^{\perp} Y = P_{\nu_{\mathcal{R}}}^{\perp} y] \\
&= \prod_{l=1}^L \mathbb{P}[S_{\mathcal{R},l}^* = s_{\mathcal{R},l}^* \mid \nu_{\mathcal{R}}^{\top} Y = t, P_{\nu_{\mathcal{R}}}^{\perp} Y = P_{\nu_{\mathcal{R}}}^{\perp} y] \\
&= \prod_{l=1}^L \mathbb{P}\left[W_{\mathcal{R},l}(s_{\mathcal{R},l}^*) - W_{\mathcal{R},l}(s) \geq G(Y; P_{\mathcal{R},l}, s) - G(Y; P_{\mathcal{R},l}, s_{\mathcal{R},l}^*), \right. \\
&\qquad\qquad\qquad \left. \forall s \in \chi_{\mathcal{R},l}^* \setminus \{s_{\mathcal{R},l}^*\} \mid \nu_{\mathcal{R}}^{\top} Y = t, P_{\nu_{\mathcal{R}}}^{\perp} Y = P_{\nu_{\mathcal{R}}}^{\perp} y \right] \\
&= \prod_{l=1}^L \mathbb{P}\left[W_{\mathcal{R},l}(s_{\mathcal{R},l}^*) - W_{\mathcal{R},l}(s) \geq G(y(t); P_{\mathcal{R},l}, s) - G(y(t); P_{\mathcal{R},l}, s_{\mathcal{R},l}^*), \forall s \in \chi_{\mathcal{R},l}^* \setminus \{s_{\mathcal{R},l}^*\} \right] \\
&= \prod_{l=1}^L \Lambda_{s_{\mathcal{R},l}^*}(t, P_{\nu_{\mathcal{R}}}^{\perp} y).
\end{aligned}$$

Here, the first display is due to the independence between the randomization variables at different splits, and as a result, we have that $S_j^* \perp\!\!\!\perp S_{j'}^* \mid Y(t) = y(t)$ for $j \neq j'$. The second display uses the description of the event in (5). The third display uses the independence between the external randomization variables and Y . We arrive at the final display by

noting that

$$(W_{\mathcal{R},l}(s_{\mathcal{R},l}^*) - W_{\mathcal{R},l}(s) : s \in \mathcal{X}_{\mathcal{R},l}^* \setminus \{s_{\mathcal{R},l}^*\}) \in \mathbb{R}^{d_l-1}$$

is distributed as a normal random variable with mean 0_{d_l-1} and covariance $\Omega_{\mathcal{R},l}$.

In the last step, letting

$$T_{s_{\mathcal{R},l}^*} = \{t \in \mathbb{R}^{d_l-1} : (t)_j \geq G(y(t); P_{\mathcal{R},l}, s) - G(y(t); P_{\mathcal{R},l}, s_{\mathcal{R},l}^*) \forall j \in [d_l - 1]\},$$

we observe that

$$\begin{aligned} & \mathbb{P}\left[W_{\mathcal{R},l}(s_{\mathcal{R},l}^*) - W_{\mathcal{R},l}(s) \geq G(y(t); P_{\mathcal{R},l}, s) - G(y(t); P_{\mathcal{R},l}, s_{\mathcal{R},l}^*), \forall s \in \mathcal{X}_{\mathcal{R},l}^* \setminus \{s_{\mathcal{R},l}^*\}\right] \\ &= \int_{T_{s_{\mathcal{R},l}^*}} \phi(u'; 0_{d_l-1}, \Omega_{\mathcal{R},l}) du' \\ &= \int_{\mathbb{R}_+^{d_l-1}} \phi\left(u; \beta_{s_{\mathcal{R},l}^*}(t, P_{\nu_{\mathcal{R}}^\perp}^\perp y), \Omega_{\mathcal{R},l}\right) du \\ &= \Lambda_{s_{\mathcal{R},l}^*}(t, P_{\nu_{\mathcal{R}}^\perp}^\perp y). \end{aligned}$$

This completes the proof. \square

Proof of Theorem 4.2. Given the conditional density of $\nu_{\mathcal{R}}^\top Y \mid \{\bar{S} = \bar{s}, P_{\nu_{\mathcal{R}}}^\perp Y = P_{\nu_{\mathcal{R}}}^\perp y\}$ in Proposition 4.2, we apply the probability integral transform (PIT) to obtain the pivot

$$P(\nu_{\mathcal{R}}^\top y, P_{\nu_{\mathcal{R}}}^\perp y; \nu_{\mathcal{R}}^\top \mu) = \frac{\int_{-\infty}^{\nu_{\mathcal{R}}^\top y} \phi(t; \nu_{\mathcal{R}}^\top \mu, \sigma^2 \|\nu_{\mathcal{R}}\|_2^2) \Lambda_{\bar{s}_{\mathcal{R}}}(t, P_{\nu_{\mathcal{R}}}^\perp y) dt}{\int_{-\infty}^{+\infty} \phi(t; \nu_{\mathcal{R}}^\top \mu, \sigma^2 \|\nu_{\mathcal{R}}\|_2^2) \Lambda_{\bar{s}_{\mathcal{R}}}(t, P_{\nu_{\mathcal{R}}}^\perp y) dt}.$$

Furthermore, because of its construct using the PIT, it follows directly that the pivot is distributed as a $\text{Unif}(0, 1)$ random variable. \square

Proof of Theorem 4.5. Consider the following four variables $V_1 = \nu_{\mathcal{R}}^\top Y, V_2 = P_{\nu_{\mathcal{R}}}^\perp Y, V_{3,l} = \{(D_{\mathcal{R},l})_k : k \in \mathcal{L}_{\mathcal{R},l}^r\}, V_{4,l} = \{(D_{\mathcal{R},l})_k : k \in \mathcal{I}_{\mathcal{R},l}^r\}$. Also, define $V_3 = (V_{3,l} : l \in [l])^\top$, and

$$V_4 = (V_{4,l} : l \in [L])^\top.$$

Treating \mathcal{R} as fixed (before conditioning), let the joint density of $(V_1, V_3, V_4)|V_2 = v_2$ at (v_1, v_3, v_4) be denoted by $q(v_1, v_3, v_4; v_2)$. Furthermore, let $q_1(v_1; v_2)$ denote the density of $V_1|V_2 = v_2$ at v_1 . Similarly, let $q_{2,l}(v_{3,l}, v_{4,l}; v_1, v_2)$ and $q_2(v_3, v_4; v_1, v_2)$ denote the densities of $(V_{3,l}, V_{4,l})|V_1 = v_1, V_2 = v_2$ and $(V_3, V_4)|V_1 = v_1, V_2 = v_2$, at the points $(v_{3,l}, v_{4,l})$ and (v_3, v_4) , respectively.

With these notations, for fixed \mathcal{R} , it holds that

$$\begin{aligned} q(v_1, v_3, v_4; v_2) &= q_1(v_1; v_2) \times q_2(v_3, v_4; v_1, v_2) \\ &= q_1(v_1; v_2) \times \prod_{l=1}^L q_{2,l}(v_{3,l}, v_{4,l}; v_1, v_2) \\ &= \underbrace{\phi(v_1; \nu_{\mathcal{R}}^\top \mu, \sigma^2 \| \nu_{\mathcal{R}} \|_2^2)}_{q_1(v_1; v_2)} \times \underbrace{\prod_{l=1}^L \phi \left(\begin{bmatrix} v_{3,l} \\ v_{4,l} \end{bmatrix}; \begin{bmatrix} \beta_{\mathcal{R},l}^1(v_1, v_2) \\ \beta_{\mathcal{R},l}^2(v_1, v_2) \end{bmatrix}, \begin{bmatrix} \Omega_{\mathcal{R},l}^{1,1} & \Omega_{\mathcal{R},l}^{1,2} \\ \Omega_{\mathcal{R},l}^{2,1} & \Omega_{\mathcal{R},l}^{2,2} \end{bmatrix} \right)}_{q_{2,l}(v_{3,l}, v_{4,l}; v_1, v_2)}. \end{aligned}$$

The first equality follows from a straightforward factorization of the joint density. The second equality uses the conditional independence of $(V_{3,l}, V_{4,l})$ given the values of (V_1, V_2) for all $l \in [L]$. Lastly, the third equality follows from the observation that

$$q_1(v_1; v_2) = \phi(v_1; \nu_{\mathcal{R}}^\top \mu, \sigma^2 \| \nu_{\mathcal{R}} \|_2^2),$$

and that

$$q_{2,l}(v_{3,l}, v_{4,l}; v_1, v_2) = \phi \left(\begin{bmatrix} v_{3,l} \\ v_{4,l} \end{bmatrix}; \begin{bmatrix} \beta_{\mathcal{R},l}^1(v_1, v_2) \\ \beta_{\mathcal{R},l}^2(v_1, v_2) \end{bmatrix}, \begin{bmatrix} \Omega_{\mathcal{R},l}^{1,1} & \Omega_{\mathcal{R},l}^{1,2} \\ \Omega_{\mathcal{R},l}^{2,1} & \Omega_{\mathcal{R},l}^{2,2} \end{bmatrix} \right)$$

Note now that we can further write

$$q_{2,l}(v_{3,l}, v_{4,l}; v_1, v_2) = g_l(v_{3,l}; v_1, v_2, v_{4,l}) \times h_l(v_{4,l}; v_1, v_2)$$

by factoring this density into the marginal density of $V_{4,l}|V_1 = v_1, V_2 = v_2$, denoted as $h_l(v_{4,l}; v_1, v_2)$, and the conditional density of $V_{3,l}|V_1 = v_1, V_2 = v_2, V_{4,l} = v_{4,l}$, denoted as $g_l(v_{3,l}; v_1, v_2, v_{4,l})$, where

$$g_l(v_{3,l}; v_1, v_2, v_{4,l}) = \phi(v_{3,l}; \beta_{s_{\mathcal{R},l}, a_{\mathcal{R},l}}^*(v_1, v_2), \Sigma_{\mathcal{R},l}), \quad h_l(v_{4,l}; v_1, v_2) = \phi(v_{4,l}; \beta_{\mathcal{R},l}^2(v_1, v_2), \Omega_{\mathcal{R},l}^{2,2}).$$

Then, for any set $I \subseteq \mathbb{R}^r$, the conditional density of

$$V_1 \mid \bigcap_{l \in [L]} \{V_2 = v_2, V_{3,l} \in I_l, V_{4,l} = v_{4,l}\},$$

at v_1 , is equal to:

$$\begin{aligned} & \frac{\phi(v_1; \nu_{\mathcal{R}}^\top \mu, \sigma^2 \|\nu_{\mathcal{R}}\|_2^2) \times \prod_{l=1}^L \int g_l(v'_{3,l}; v_1, v_2, v_{4,l}) h_l(v_{4,l}; v_1, v_2) \mathbb{1}[v'_{3,l} \in I_l] dv'_{3,l}}{\int \phi(v'_1; \nu_{\mathcal{R}}^\top \mu, \sigma^2 \|\nu_{\mathcal{R}}\|_2^2) \times \int \prod_{l=1}^L g_l(v'_{3,l}; v'_1, v_2, v_{4,l}) h_l(v_{4,l}; v'_1, v_2) \mathbb{1}[v'_{3,l} \in I_l] dv'_{3,l} dv'_1} \\ & \propto \phi(v_1; \nu_{\mathcal{R}}^\top \mu, \sigma^2 \|\nu_{\mathcal{R}}\|_2^2) \times \prod_{l=1}^L h_l(v_{4,l}; v_1, v_2) \times \int g_l(v'_{3,l}; v_1, v_2, v_{4,l}) \mathbb{1}[v'_{3,l} \in I_l] dv'_{3,l} \\ & = \phi(v_1; \nu_{\mathcal{R}}^\top \mu, \sigma^2 \|\nu_{\mathcal{R}}\|_2^2) \times \prod_{l=1}^L \phi(v_{4,l}, \beta_{\mathcal{R},l}^2(v_1, v_2), \Omega_{\mathcal{R},l}^{2,2}) \\ & \quad \times \mathbb{P}[V_{3,l} \in I_l \mid V_1 = v_1, V_2 = v_2, V_{4,l} = v_{4,l}]. \end{aligned} \tag{6}$$

At last, note that our conditional density of interest,

$$\nu_{\mathcal{R}}^\top y \mid \bar{S}_{\mathcal{R}} = \bar{s}_{\mathcal{R}}, \bar{A}_{\mathcal{R}} = \bar{a}_{\mathcal{R}}, P_{\nu_{\mathcal{R}}}^\perp Y = P_{\nu_{\mathcal{R}}}^\perp y,$$

using the notations in the proof, is equal to the conditional density of

$$V_1 \mid \bigcap_{l \in [L]} \left\{ V_2 = P_{\nu_{\mathcal{R}}}^\perp y, V_{3,l} \in H_{\mathcal{R},l}^{(r)}, V_{4,l} = \mathcal{D}_{\mathcal{R},l}^{(r)} \right\}$$

where $H_{\mathcal{R},l}^{(r)} = \{u \in \mathbb{R}^r : 0 < u_k < [D_{\mathcal{R},l}]_{(r+1)} \text{ for } k \in [r]\}$. This density, at $t \in \mathbb{R}$, based on our calculations in (6), equals

$$\phi(t; \nu_{\mathcal{R}}^\top \mu, \sigma^2 \|\nu_{\mathcal{R}}\|_2^2) \times \prod_{l=1}^L \phi(\mathcal{D}_{\mathcal{R},l}^{(r)}, \beta_{\mathcal{R},l}^2(t, P_{\nu_{\mathcal{R}}}^\perp y), \Omega_{\mathcal{R},l}^{2,2}) \times \int_{H_{\mathcal{R},l}^{(r)}} \phi(u; \beta_{s_{\mathcal{R},l}^*, a_{\mathcal{R},l}}(t, P_{\nu_{\mathcal{R}}}^\perp y), \Sigma_{\mathcal{R},l}) du.$$

Applying the PIT to this conditional density yields the claimed pivot.

□

B Pivot under adaptive stopping rules

Although the primary inferential results in Section 4 were developed for fixed-depth trees or more generally, trees grown using deterministic stopping rules, we demonstrate here that our RRT method can be extended to accommodate other TREE-models grown with adaptive stopping rules. This is achieved by making slight modifications to the standard rules with external randomization. Specifically, we discuss randomized variants of two commonly used adaptive stopping rules. For both types of adaptively grown TREE-models, we show how inference for the data-dependent model parameters can be conducted using a similar approach as developed for the fixed-depth trees in Section 4.

Rule based on thresholding the gain function. Consider growing the classic regression tree, $TREE^\lambda(Y; X)$, without external randomization, in the following manner. At a region $P_k \subset \mathbb{R}^p$, we first select the split $s_k^* \in \mathcal{X}_{P_k}$ that maximizes the gain function $G(Y; P_k, s)$;

but, the split is made only if the gain $G(Y; P_k, s_k^*)$ exceeds a pre-specified threshold λ ; otherwise, we stop.

To grow $TREE^\lambda(Y, \overline{W}; X)$ with added randomization variables, we apply the same rule, but this time to the randomized gain functions rather than the standard gain function. More precisely, at the parent region $P_k \subset \mathbb{R}^p$, we observe $\{S_k^*(Y, \overline{W}_k; P_k) = s_k^*\}$ if and only if

$$\left\{ s_k^* = \arg \max_{s \in \chi_k} G(Y; P_k, s) + W_k(s) \right\} \cap \left\{ G(Y; P_k, s_k^*) + W_k(s_k^*) \geq \lambda \right\} \quad (7)$$

where $\overline{W}_k = \{W_k(s), s \in \chi_k\}$ are randomization variables drawn independently from $\mathcal{N}(0, \tau_{P_k}^2)$ and also independent of Y . Algorithm 2 summarizes the steps to build an adaptively grown TREE-model using this randomized thresholding rule.

To address inference with this adaptive stopping rule, note that the event in (7) is equivalent to

$$\left\{ W_k(s_k^*) - W_k(s) \geq G(Y; P_k, s) - G(Y; P_k, s_k^*), \forall s \in \chi_k \setminus \{s_{\mathcal{R},1}^*\} \right\} \\ \cap \left\{ W_k(s_k^*) \geq \lambda - G(Y; P_k, s_k^*) \right\}.$$

For the series of L selected splits $\overline{s}_{\mathcal{R}} = \{s_{\mathcal{R},1}^*, s_{\mathcal{R},2}^*, \dots, s_{\mathcal{R},L}^*\}$ in the sub-tree leading to the terminal region \mathcal{R} , define for each $l \in [L]$:

$$O_{s_{\mathcal{R},l}^*}^{(1)}(t, P_{\nu_{\mathcal{R}}}^\perp y) = \left(G(y(t); P_{\mathcal{R},l}, s_{\mathcal{R},l}^*) - \lambda, \beta_{s_{\mathcal{R},l}^*}(t, P_{\nu_{\mathcal{R}}}^\perp y) \right)^\top$$

where $y(t)$ and $\beta_{s_{\mathcal{R},l}^*}(t, P_{\nu_{\mathcal{R}}}^\perp y)$ are as defined before.

Then, for $\tilde{\Omega}_{\mathcal{R},l}^{(1)} = \begin{bmatrix} \tau_{P_{\mathcal{R},l}}^2 & \tau_{P_{\mathcal{R},l}}^2 \cdot \mathbf{1}_{d_l-1}^\top \\ \tau_{P_{\mathcal{R},l}}^2 \cdot \mathbf{1}_{d_l-1} & \Omega_{\mathcal{R},l} \end{bmatrix} \in \mathbb{R}^{d_l \times d_l}$, we define

$$\tilde{\Lambda}_{s_{\mathcal{R},l}^*}^{(1)}(t, P_{\nu_{\mathcal{R}}}^\perp y) = \int_{\mathbb{R}_+^{d_l}} \phi\left(u; O_{s_{\mathcal{R},l}^*}^{(1)}(t, P_{\nu_{\mathcal{R}}}^\perp y), \tilde{\Omega}_{d_l}^{(1)}\right) du.$$

In Theorem B.1, we present our pivot for inference in the TREE-model, derived from the output of Algorithm 2.

Theorem B.1. *Given data $Y = y$, a pivot for $\nu_{\mathcal{R}}^\top \mu$ equals*

$$P^{(1)}(\nu_{\mathcal{R}}^\top y, P_{\nu_{\mathcal{R}}}^\perp y; \nu_{\mathcal{R}}^\top \mu) = \frac{\int_{-\infty}^{\nu_{\mathcal{R}}^\top y} \phi(t; \nu_{\mathcal{R}}^\top \mu, \sigma^2 \|\nu_{\mathcal{R}}\|_2^2) \tilde{\Lambda}_{\bar{s}_{\mathcal{R}}}^{(1)}(t, P_{\nu_{\mathcal{R}}}^\perp y) dt}{\int_{-\infty}^{+\infty} \phi(t; \nu_{\mathcal{R}}^\top \mu, \sigma^2 \|\nu_{\mathcal{R}}\|_2^2) \tilde{\Lambda}_{\bar{s}_{\mathcal{R}}}^{(1)}(t, P_{\nu_{\mathcal{R}}}^\perp y) dt},$$

which, conditional on $\{\bar{S} = \bar{s}\}$, is distributed as a $\text{Unif}(0, 1)$ random variable.

The proof of Theorem B.1 closely resembles the proof for deriving the pivot related to the adaptive stopping rule based on cost complexity, which we will discuss next. Therefore, we will provide the proof for both of these pivots in the following section.

Rule based on a cost complexity criterion. Another commonly used adaptive stopping rule is based on a cost-complexity strategy, which in the standard CART is also employed for bottom-up pruning. This approach removes all descendants of a region P if the gain in the sum of squared errors based on the terminal regions of P is less than a pre-specified, cost-complexity threshold λ . That is, let $\text{TERM}(P)$ be the set of all terminal nodes with P as parent. The decision to not further split region P is made if the average gain in MSE, defined as

$$\text{GM}(Y; P) = \frac{\sum_{i: X_i \in P} (Y_i - \bar{Y}_P)^2 - \sum_{R \in \text{TERM}(P)} \sum_{i: X_i \in R} (Y_i - \bar{Y}_R)^2}{|\text{TERM}(P)| - 1}$$

Algorithm 2 Randomized CART: TREE growing algorithm with adaptive stopping 1

- 1: **Input:** Training data (X, Y) , maximum depth d_{\max} , pruning parameter λ
- 2: **Initialize:** Root region $P_1 = \mathbb{R}^p$, current depth $d = 0$
- 3: **for** each region P with $n_P > 1$ samples at depth $d < d_{\max}$ **do**
- 4: Draw a data-independent randomization $W(s) \sim \mathcal{N}(0, \tau_P^2)$ for all $s \in \chi_P$
- 5: Compute the gain function $G(Y; P, s)$ for all possible splits $s = (j, o) \in \chi_P$
- 6: Select the split s^* with the maximum randomized gain:

$$s^* = \operatorname{argmax}_{s \in \chi_P} G(Y; P, s) + W(s)$$

- 7: **if** $G(Y; P, s^*) + W(s^*) \geq \lambda$ **then**
 - 8: Partition P based on selected split into $\{P_{s^*}^l, P_{s^*}^g\}$
 - 9: depth $d \leftarrow d + 1$
 - 10: **else**
 - 11: Return P as a terminal region
 - 12: **end if**
 - 13: **end for**
-

does not exceed the complexity threshold λ . The RRT can incorporate a similar adaptive stopping rule with external randomization.

Similar to the previous rule, we modify the splitting criterion by using a randomized version of the function $\text{GM}(Y; P)$. Consider the parent region $P_k \subset \mathbb{R}^p$ in our RRT. First, we apply the standard CART algorithm with a fixed depth d_0 , using P_k as the root node, and compute $\text{GM}(Y; P_k)$, based on the terminal regions of the CART output. Then, in our RRT, we observe $\{S_k^*(Y, \overline{W}_k; P_k) = s_k^*\}$ if and only if

$$\left\{ s_k^* = \operatorname{argmax}_{s \in \chi_k} G(Y; P_k, s) + W_k(s) \right\} \cap \left\{ \text{GM}(Y; P_k) + \widetilde{W}_k \geq \lambda \right\}, \quad (8)$$

where $\overline{W}_k = \left\{ W_k(s), s \in \chi_k \right\} \cup \left\{ \widetilde{W}_k \right\}$ are $d_k + 1$ data independent randomization terms drawn from $\mathcal{N}(0, \tau_{P_k}^2)$. This adaptive variant of the RRT is outlined in Algorithm 3. Ob-

viously, the event in (8) is equivalent to

$$\left\{ W_k(s_k^*) - W_k(s) \geq G(Y; P_k, s) - G(Y; P_k, s_k^*), \quad \forall s \in \chi_k \setminus \{s_k^*\} \right\} \\ \cap \left\{ \text{GM}(Y; P_k) + \widetilde{W}_k \geq \lambda \right\}.$$

Algorithm 3 Randomized CART: TREE growing algorithm with adaptive stopping 2

- 1: **Input:** Training data (X, Y) , maximum depth d_{\max} , pruning parameter λ
- 2: **Initialize:** Root region $P_1 = \mathbb{R}^p$, current depth $d = 0$
- 3: **for** each region P with $n_P > 1$ samples at depth $d < d_{\max}$ **do**
- 4: Draw data-independent randomization $\left\{ \{W(s) : s \in \chi_P\}, \widetilde{W} \right\} \stackrel{i.i.d.}{\sim} \mathcal{N}(0, \tau_P^2)$
- 5: Compute the gain function $G(Y; P, s)$ for all possible splits $s = (j, o) \in \chi_P$
- 6: Select the split s^* with the maximum randomized gain:

$$s^* = \underset{s \in \chi_P}{\operatorname{argmax}} G(Y; P, s) + W(s)$$

- 7: Grow a d_{\max} depth CART tree from P , say has terminal regions $\text{TERM}(P)$ then calculate $\text{GM}(Y; P)$
 - 8: **if** $\text{GM}(Y; P) + \widetilde{W} \geq \lambda$ **then**
 - 9: Partition P based on selected split into $\{P_{s^*}^l, P_{s^*}^g\}$
 - 10: depth $d \leftarrow d + 1$
 - 11: **else**
 - 12: Return P as a terminal region
 - 13: **end if**
 - 14: **end for**
-

Consider observing $\bar{s}_{\mathcal{R}} = \{s_{\mathcal{R},1}^*, s_{\mathcal{R},2}^*, \dots, s_{\mathcal{R},L}^*\}$. Using the notations introduced earlier, define for each $l \in [L]$:

$$O_{s_{\mathcal{R},l}^*}^{(2)}(t, P_{\nu_{\mathcal{R}}}^\perp y) = \left(\text{GM}(Y; P_{\mathcal{R},l}) - \lambda, \beta_{s_{\mathcal{R},l}^*}(t, P_{\nu_{\mathcal{R}}}^\perp y) \right)^\top.$$

For $\tilde{\Omega}_{\mathcal{R},l}^{(2)} = \begin{bmatrix} \tau_{P_{\mathcal{R},l}}^2 & 0_{d_{l-1}}^\top \\ 0_{d_{l-1}} & \Omega_{\mathcal{R},l} \end{bmatrix} \in \mathbb{R}^{d_l \times d_l}$, let

$$\tilde{\Lambda}_{s_{\mathcal{R},l}^*}^{(2)}(t, P_{\nu_{\mathcal{R}}}^\perp y) = \int_{\mathbb{R}_+^{d_l}} \phi(u; O_{s_{\mathcal{R},l}^*}^{(2)}(t, P_{\nu_{\mathcal{R}}}^\perp y), \Omega_{\mathcal{R},l}^{(2)}) du.$$

In Theorem B.2, we provide a pivot for inference in the TREE-model, based on the output of Algorithm 3.

Theorem B.2. *Given data $Y = y$, a pivot for $\nu_{\mathcal{R}}^\top \mu$ equals*

$$P^{(2)}(\nu_{\mathcal{R}}^\top y, P_{\nu_{\mathcal{R}}}^\perp y; \nu_{\mathcal{R}}^\top \mu) = \frac{\int_{-\infty}^{\nu_{\mathcal{R}}^\top y} \phi(t; \nu_{\mathcal{R}}^\top \mu, \sigma^2 \|\nu_{\mathcal{R}}\|_2^2) \tilde{\Lambda}_{\bar{s}_{\mathcal{R}}}^{(2)}(t, P_{\nu_{\mathcal{R}}}^\perp y) dt}{\int_{-\infty}^{+\infty} \phi(t; \nu_{\mathcal{R}}^\top \mu, \sigma^2 \|\nu_{\mathcal{R}}\|_2^2) \tilde{\Lambda}_{\bar{s}_{\mathcal{R}}}^{(2)}(t, P_{\nu_{\mathcal{R}}}^\perp y) dt},$$

which, conditional on $\{\bar{S} = \bar{s}\}$, is distributed as a $\text{Unif}(0, 1)$ random variable.

Proofs of Theorem B.1 and B.2. Using the same strategy as adopted for the proof of Theorem 4.2, the conditional density of $\nu_{\mathcal{R}}^\top Y \mid \{\bar{S} = \bar{s}, P_{\nu_{\mathcal{R}}}^\perp Y = P_{\nu_{\mathcal{R}}}^\perp y\}$, when evaluated at $t \in \mathbb{R}$ is proportional to

$$\phi(t; \mu_{\mathcal{R}}, \sigma^2 \|\nu_{\mathcal{R}}\|_2^2) \times \mathbb{P}[\bar{S}_{\mathcal{R}} = \bar{s}_{\mathcal{R}} \mid P_{\nu_{\mathcal{R}}}^\perp Y = P_{\nu_{\mathcal{R}}}^\perp y, \nu_{\mathcal{R}}^\top Y = t].$$

Now it remains to compute

$$\mathbb{P}[\bar{S}_{\mathcal{R}} = \bar{s}_{\mathcal{R}} \mid P_{\nu_{\mathcal{R}}}^\perp Y = P_{\nu_{\mathcal{R}}}^\perp y, \nu_{\mathcal{R}}^\top Y = t].$$

To do so, define

$$Z_{\mathcal{R},l}^{(1)} = (G(Y; P_{\mathcal{R},l}, s_{\mathcal{R},l}^*) + W_{\mathcal{R},l}(s_{\mathcal{R},l}^*) - \lambda, D_{\mathcal{R},l})^\top; \quad Z_{\mathcal{R},l}^{(2)} = (\text{GM}(Y; P) + \widetilde{W}_{\mathcal{R},l} - \lambda, D_{\mathcal{R},l})^\top$$

The proofs of Theorem B.1 and B.2 follow the same steps as before, as shown in Proposition 4.2, utilizing the fact that

$$Z_{\mathcal{R},l}^{(1)} | Y = y(t) \sim \mathcal{N} \left(O_{s_{\mathcal{R},l}^*}^{(1)}(t, P_{\nu_{\mathcal{R}}}^\perp y), \tilde{\Omega}_{\mathcal{R},l} \right), \quad Z_{\mathcal{R},l}^{(2)} | Y = y(t) \sim \mathcal{N} \left(O_{s_{\mathcal{R},l}^*}^{(2)}(t, P_{\nu_{\mathcal{R}}}^\perp y), \tilde{\Omega}_{\mathcal{R},l} \right)$$

and

$$\{\bar{S}_{\mathcal{R}} = \bar{s}_{\mathcal{R}}\} = \left\{ Z_{\mathcal{R},l}^{(k)} > 0 \text{ for } l \in [L] \right\}$$

by setting $k = 1, 2$ respectively for the two adaptive rules. □

C Additional simulations

Results under varying Laplace noise scales In this experiment, we investigate the robustness of the proposed method, as well as the baseline methods, to misspecification of the noise distribution. We set $D = \text{Laplace}(0, \sigma_L/\sqrt{2})$, for $\sigma_L \in \{1, 2, 5, 10\}$, such that $\text{SD}(\epsilon_i) \in \{1, 2, 5, 10\}$. We set the dimension $p = 10$.

Following this, we compute selective inference using our proposed method and the other two baseline methods and report the results obtained from 500 simulations. The resulting coverage rates, average confidence interval lengths, and test MSE are presented in Figure 6.

We note that similar trends are observed, even under a misspecified noise distribution: all three methods approximately achieve the targeted coverage rate of 90%, and the proposed method produces confidence intervals that are shorter than Tree-values intervals by orders of magnitude, and shorter than or comparable to UV intervals in terms of lengths, with the proposed method having favorable test MSE performance compared to the two baseline methods.

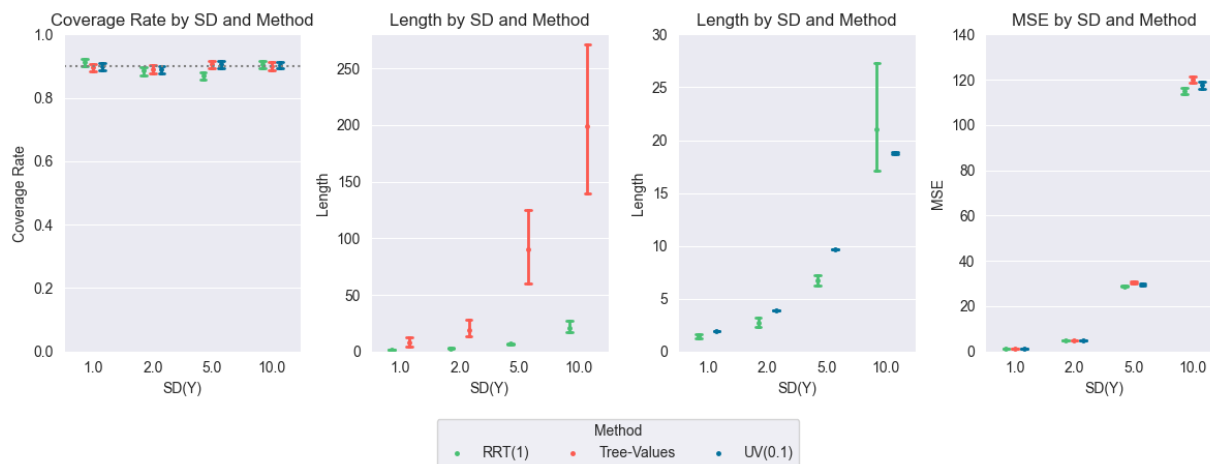


Figure 6: Coverage rate, average CI length, and prediction MSE of RRT(1), Tree-Values, and the UV method for $\sigma_L^2 \in \{1, 2, 5, 10\}$ and Laplace noise; The dotted line is plotted at 0.9 in the coverage plot

D Additional details for the PROMPT study

	Description
ActivityCalories	Calories burned from periods above sedentary level, personal average
BodyBmi	Body Mass Index, from the Body Time Series, personal average
BodyWeight	Body weight, from the Body Time Series, personal average
Calories	Calories, from the Activity Time Series, personal average
CaloriesBMR	Only BMR (Basal Metabolic Rate) calories, from the Activity Time Series, personal average
Distance	Distance traveled, from the Activity Time Series, personal average
HeartRateIntradayCount	The number of intraday heart rate samples collected during the time period, personal average
ActivityCaloriesSD	Calories burned from periods above sedentary level, personal sd
CaloriesSD	Calories, from the Activity Time Series, personal average, personal sd
CaloriesBMR_SD	Only BMR (Basal Metabolic Rate) calories, from the Activity Time Series, personal sd
DistanceSD	Distance traveled, from the Activity Time Series, personal average, personal sd
HeartRateIntradayCountSD	The number of intraday heart rate samples collected during the time period, personal sd
ASSIST_B	The Alcohol, Smoking and Substance Involvement Screening Test score at baseline (intake) survey
GAD_B	General Anxiety Disorder Survey score at baseline (intake) survey
ISEL_B	Interpersonal Support Evaluation List score at baseline (intake) survey
NEO_B	NEO Personality Inventory score at baseline (intake) survey
PANSL_B	Positive and Negative Suicide Ideation score at baseline (intake) survey
PCL_B	PTSD Checklist score at baseline (intake) survey
PHQ_B	Patient Health Questionnaire score at baseline (intake) survey
PSQLB	Pittsburgh Sleep Quality Index score at baseline (intake) survey
RFQ_B	The Reflective Functioning Questionnaire score at baseline (intake) survey
PHQ (response variable)	Patient Health Questionnaire score at 6-week survey

Table 4: Documentation for variables included in the PROMPT analysis